ISOFORMS, SUBCELLULAR LOCALIZATION AND ROLE IN SURVIVAL FOR MAMMALIAN ENDONUCLEASE V

ISOFORMER, SUBCELLULÆR LOKALISERING OG ROLLE I OVERLEVELSE FOR MAMMALSK ENDONUKLEASE V

EIRIK THORGAARD

Norwegian University of Life Sciences
Department of Chemistry, Biotechnology and Food Science
Master Thesis 60 credits 2012

Acknowledgements

This thesis concludes my Master degree at the Department of Chemistry, Biotechnology and Food Science, Norwegian University of Life Sciences. The laboratory part of this study was carried out externally at Department of Microbiology, Section for Research, Oslo University Hospital, Rikshospitalet during the period February 2011 – May 2012.

First of all I would like to thank my supervisors, group leader Prof. Magnar Bjørås, Dr. Cathrine Fladeby and Dr. Ingrun Alseth at Rikshospitalet, and my internal supervisor Prof. Dzung Bao Diep at the Department of Chemistry, Biotechnology and Food Science, Norwegian University of Life Sciences for making this project feasible.

I would special like to thank Cathrine Flade and Ingrun Alseth for always having time to answer my questions and for trusting me with challenging work. I am especially grateful for theirs invaluable help with the writing of this thesis. Thank you both for sharing yours impressively amount of knowledge, and for being patient and inspiring supervisors.

In addition, I would like to thank my colleagues at the Yeast group. They included me in interesting discussions of their projects and made me look forward to every day in the lab.

Finally I would like to thank my family and friends for all encouragement during my thesis. A special thanks to Stiann Jeff Fiquet Bredesen for all moral support, and for believing in me.

Oslo, May 2012

_____

Eirik Thorgaard

Abstract

Our hereditary material, the DNA, is on a daily basis subjected to endogenous and exogenous agents that lead to DNA damage. Therefore it is essential for the genomic integrity that these damages are repaired efficiently. As a response to DNA damage, cells have developed various repair mechanisms and defects in these are associated with cancer, ageing, and various neurodegenerative diseases. Therefore it is important to understand how the DNA is repaired and how the genetic information is preserved. A broader understanding of the DNA repair enzymes and how they function is an important matter.

Endonuclease V (EndoV) is a highly conserved DNA repair enzyme found in most organisms from prokaryotes to human. Prokaryotic EndoV has affinity for deaminated bases in DNA. *Escherichia coli* EndoV recognizes and binds to deaminated adenine (hypoxanthine), and cleaves the DNA stand at the second phosphodiester bond 3' of the lesion. The high degree of conservation in the EndoV family suggests an important function also in the eukaryotic cell. The aim of this thesis has been to characterize the endonuclease V homologs from *Homo sapiens* and *Mus musculus.*

The results from this study show that there are a high (and uncertain) number of isoforms of human ENDOV, which makes it difficult to characterize and determine the function of this protein. The full-length *hENDOV* transcript (exon 3-contaning) does not represent the majority of the transcript variants in human cells, which is unexpected since exon 3 is known to make up the core of the protein. In line with this, endogenous full-length hENDOV protein could not be detected, neither in Western analysis or by immunoprecipitation.

Intracellular localisation of hENDOV fused to EGFP showed that isoform 1 was located to the cytoplasm and nucleus with enrichment in nucleoli in transfected HeLa-S3 cells, whereas the other two isoforms showed only localization in the cytoplasm. Cells expressing hENDOV isoform 1 was exposed to DNA damaging agents, and interestingly, after CPT exposure hENDOV was excluded from the nucleoli. The role of hENDOV in the nucleoli remains unclear.

The viability assay (MTT-assay) on primary mouse embryonic fibroblast (MEF) cell lines with or without *mEndoV* revealed no difference in survival after treatment with DNA damaging agents.

In summary, this thesis presents the first the characterization of the human ENDOV protein. Despite high conservation in all domains of life and current results, the function of mammalian EndoV is still unclear and further studies are needed.

Sammendrag

Arvestoffet vårt, DNA, utsettes daglig for endogene og eksogene forbindelser som fører til ulike skader. Effektiv reparasjon av skadene er essensielt for å opprettholde genomets integritet. Cellene har utviklet ulike reparasjonsmekanismer, som involverer mange forskjellige enzymer, som respons på DNA skadene. Feil eller mangler i reparasjonsmekanismene er assosiert med kreft, aldring og ulike neurodegenererende sykdommer. En større forståelse av enzymene som deltar og hvordan de fungerer er viktig for å forstå hvordan DNA blir reparert og hvordan den genetiske informasjonen bevares.

Endonuklease V (EndoV) er et svært konservert gen fra prokaryoter til mennesker. Prokaryotisk EndoV har en substratspesifisitet for deaminated baser i DNA. *Escherichia coli* EndoV gjenkjenner og binder til deaminert adenin (hypoxantin) og kutter den andre fosfodiester binding på DNA tråden på 3' side av skaden. Siden EndoV er godt konservert antas at dette proteinet har en viktig funksjon i eukaryotiske celler. Formålet med denne oppgaven har vært å karakterisere funksjonen til endonuklease V i fra *Homo sapiens* og *Mus musculus*

Resultatene fra denne studien viser at det er et høyt (og usikre) antall isoformer av human ENDOV, noe som gjør det vanskelig å karakterisere og bestemme funksjonen til dette proteinet. I humane celler kan det virke som at de fleste transkripter mangler ekson 3. Dette er overraskende, siden ekson 3 tilsvarer kjernen av proteinet. Det ble heller ikke detektert endogent hENDOV i celle lysat ved immunopresipitering.

Intracellulær lokalisering av hENDOV isoform 1 fusjonert med EGFP, ble lokalisert til cytoplasma og i nukleus med anrikning i nukleoli i transfekterte HeLa-S3 celler. De to andre isoformene viste kun lokalisering i cytoplasma. Etter eksponering med det DNA-skadene stoffet CPT, ble hENDOV isoform 1 eksludert fra nucleoli, men rollen for hENDOV i nukleoli er fortsatt uklar.

MTT-assayene på cellelinjene av primære muse embryonale fibroblast (MEF) viste ingen forskjell i overlevelse etter behandling med DNA skadene agens mellom de cellelinjene hvor genet for *mEndoV* har blitt slått ut, mot de cellelinjene der genet fortsatt var intakt.

Kort oppsummert, presenterer denne oppgaven er den første karakteriseringen av den humane ENDOV protein. Til tross for den høye graden av konserveringen i pattedyr, er funksjonen av mammalsk EndoV fortsatt uklart så videre studier er nødvendig.

Table of contents

Abbreviations

8-oxoG	7,8-dihydro-8-oxoguanine
A	Adenine
aa	Amino acid
ALKBH	AlkB homolog
Apn1	Apurine endonuclease I
AP-site	Apurinic/apyrimidinic site
ATLD	AT-like disorder (ATLD)
BER	Base excision repair
bp	Base pairs
BSA	Bovine serum albumin
C	Cytosine
CAA	Chloroacetaldehyde
cDNA	Complementary DNA
CS	Cockayne's syndrome
DNA	Deoxyribonucleic acid
dNTP	Deoxyribonucleotide triphosphate
dRP	5'-deoxyribose phosphatase
DSB	Double-stand break
DTT	Dithiothreitol
E. coli	*Escherichia coli*
EcEndoV	*E. coli* Endonuclease V
EDTA	Ethylenediaminotetraacetic acid
Embryonic stem	ES
EndoV	Endonuclease V
EST	Expressed sequence tags

ExoI	Exonuclease I
faPy	Formamidopyrimidines
FEN1	Flap endonuclease 1
G	Guanine
g	G-force
GGR	Global genome repair
HCl	Hydrochloric acid
hENDOV	Human Endonuclease V
HNO_2	Nitrous acid
HNPCC	Hereditary nonpolyposis colorectal cancer (HNPCC)
HR	Homologous recombination
I	Inosine
Lig I	DNA ligase I
Lig III	DNA ligase III
M. musculus	*Mus musculus*
M/R/N	Mre11/Rad50/NBS1
mEndoV	Mouse Endonuclease V
MGMT	O^6-methylguanine DNA methyltransferase
MMR	Mismatch repair
MMS	Methyl methanesulfonate
MOPS	3-(N-morfolino) propanesulfonate
MQ H_2O	MilliQ filtered and ion-exchange water
mRNA	Messenger RNA
MTT	3-[4, 5-dimethylthiazol-2-yl]-2, 5-diphenyl tetrazolium bromide
N	Nitrogen
NBS	Nijmegen breakage syndrome (NBS)
NER	Nucleotide excision repair
nfi	E. coli Endonuclease V

Nfo	*E. coli* endonuclease IV
NHEJ	Non-homologous DNA end-joining
NIR	Nucleotide incision repair
O	Oxygen
O_2^- •	Superoxide anion
OD	Optical density
OH •	Hydroxyl radical
PAGE	Polyacrylamide gel electrophoresis
PBS	Phosphate buffer saline
PBS-T	Phosphate buffer saline - Tween® 20
PCNA	Proliferating cellular nuclear antigen
PCR	Pilymerase chain reaction
Polβ	DNA polymerase β
PYIP	Pro79-Tyr80-Ile81-Pro82
RefSeq	NCBI Reference Sequence
RNA	Ribo nucleic acid
ROS	Reactive oxygen species
RPA	Replication protein A
RT	Room temperature
S. cerevisiae	*Saccharomyces cerevisiae*
S. pombe	*Schizosaccharomyces pombe*
SAM	S-adenosyl-methionine
SDS	Sodium dodecyl sulphate
SNP	Single-nucleotide polymorphisms
SSA	Single-strand annealing
SSB	Single-strand breaks
ssDNA	Single-stranded DNA
T	Thymine

T. maritima	*Thermotoga maritima*
TBE	Tris borate EDTA
TCR	Transcription coupled repair
THF	Tetrahydrofuran
TmaEndoV	*Thermotoga maritima* Endonuclease V
Tris	Tris(hydroxymethyl)aminomethane
TTD	Trichothiodystrophy
U	Uracil
UV	Ultraviolet
XP	Xeroderma pigmentosum
XRCC1	X-ray repair cross complementing 1 protein

1 Introduction

Deoxyribonucleic acid (DNA) is the carrier of the genetic information and contains the instructions for the development and functioning of living organisms. Maintenance of the genome is therefore crucial for life. A variety of both exogenous and endogenous reactive compounds present a constant threat to the integrity of the DNA in living cells. To cope with the frequent challenge of endogenous and exogenous DNA insult, all eukaryotic cells have evolved a versatile DNA damage response (Figure 1.1). When DNA damage is detected, cell cycle checkpoint are activated to arrest cell cycle progression so that the DNA can be repaired before being passed to daughter cells (Nyberg *et al.* 2002;Hakem 2008). In addition to checkpoint activation, transcriptional programs are induced and if the level of damage is severe, apoptosis is initiated. To ensure that the genetic material is properly maintained, duplicated, and segregated within the cell, all the above processes are carefully coordinated. Defects in the DNA damage response and DNA repair processes have been shown to be involved in genetically inherited disorders, in ageing, and in carcinogenesis, and these findings underscore the importance of intact DNA checkpoint regulation and DNA repair for proper function and survival of the organism (Hoeijmakers 2001;Thoms *et al.* 2007;Hakem 2008;Altieri *et al.* 2008).

The sources of DNA damaging agents may be exogenous (sunlight, tobacco smoke and food constituents), or endogenous (water and reactive oxygen species (ROS)). They may induce different types of DNA damage, ranging from single base alterations to bulky helix-distorting lesions and single- and double-strand DNA breaks (SSB/DSB) (Barnes and Lindahl 2004). DNA repair is probably the most important cellular mechanism against these modifications and hence the development of cancer and neurodegenerative diseases. This is illustrated by rare syndromes like Cockayne's syndrome (CS), the Xeroderma pigmentosum (XP) syndrome and Trichothiodystrophy (TTD) caused by defective DNA repair and whose patients are prone to cancer and neurodegeneration. To facilitate therapeutic methods in addition to preventative strategies for these diseases, the knowledge of how the human organism preserves genomic integrity is crucial.

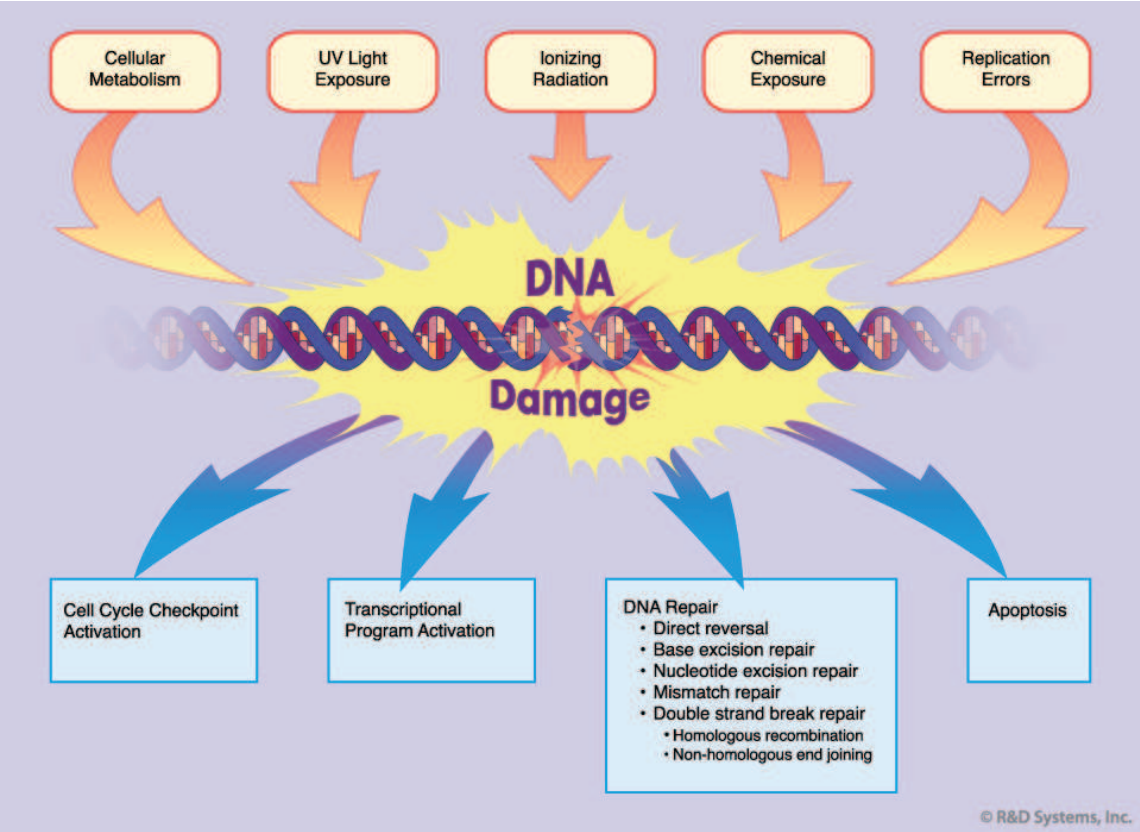

Figure 1.1. The DNA damage response. DNA damage is caused by a variety of sources. The cellular response to damage may involve activation of a cell cycle checkpoint, initiation of transcriptional programs, and induction of DNA repair or apoptosis (adapted from: http://rndsystems.com/mini_review_detail_objectname_MR03_DNADamageResponse.aspx).

1.1 DNA damage

1.1.1 Oxidative DNA damage

All mammals use oxygen as a life giving source, but paradoxically this molecule can also inflict huge problems for the organism. Normal aerobic metabolism generates oxygen metabolites called ROS that can attack intracellular macromolecules such as lipids, proteins and nucleic acids. ROS is also a result exogenous compounds such as UV radiation, chemicals (such as herbicides, algaecides, fungicides, bactericides, and viricides), and cigarette smoke (Kow 1999;Maynard et al. 2009). Free radicals are defined as species component of independent existence that contains one or more unpaired valence shell electron. Other common ROS compounds: the highly reactive hydroxyl radical (OH •), superoxide anion (O_2^- •) and the non-radical H_2O_2 (Burney et al. 1999;Maynard et al. 2009) . The cells can prevent the damage inflicted by free radicals with antioxidants, which are compounds that inactivate oxidants to less reactive compounds. As previously mentioned free

radicals can damage lipids, proteins and RNA, but these molecules can, unlike DNA, the cell can created new of if they are damaged (Kow 1999;Maynard et al. 2009). One prominent damage coused by ROS on DNA is 7,8-dihydro-8-oxoguanine (8-oxoG) (Slupphaug et al. 2003). This base lesion can form a Hoogsteen base pair with adenine during replication, and will lead to a G:C to T:A transversion mutation if not repaired (Kirouac and Ling 2011). Other dominant damages to DNA are ring-opened formamidopyrimidines (faPy), hydroxycytosine, and thymine glycol (Slupphaug et al. 2003).

1.1.2 DNA deamination

Hydrolytic deamination of DNA is the spontaneous removal of an amine group from a DNA base (Lindahl 1993). The amino group is then replaced by a keto group that give the bases other properties. The deamination can be greatly enhanced by ROS, ionizing radiation, and nitrous acid (HNO_2) (Kow 2002). Cytosine, adenine, guanine, and 5-methylcytosine can be deaminated to form uracil, hypoxanthine, xanthine, and thymine, respectively (Shapiro and Shiuey 1969;Kow 2002). Deaminated cytosine, uracil, will produce G:U mismatches that results in G:C → A:T transition mutations following replication (Schouten and Weiss 1999;Barnes and Lindahl 2004). U:G mismatches are recognized by *E. coli* Endonuclease V (EcEndoV) (Gates and Linn 1977). The deamination product, hypoxanthine, can also be repaired by two different enzymes, the alkylbase DNA glycosylase, AlkA, which initiates repair by removal of the damaged base and EndoV. EndoV initiates repair by hydrolyses the second phosphodiester bond 3' to the lesion (Saparbaev and Laval 1994;Schouten and Weiss 1999). The corresponding nucleoside hypoxanthine is called inosine. Lindahl and Nyberg showed in 1974 that the heat induction hydrolytic deamination of cytosine occurs to a much greater extent in single-stranded DNA than double-stranded DNA. This is due to the helix structure of double-stranded DNA that protects residues from being deaminated (Barnes and Lindahl 2004).

1.1.3 Alkylated damage DNA

Alkylating agents are formed endogenously as well as being widely present in the environment in food, cigarette smoke, chemicals, and chemotherapeutic (Sedgwick 2004). An important alkylating agent is the cellular methyl donor S-adenosyl-methionine (SAM) (Barrows and Magee 1982;Rydberg and Lindahl 1982;Naslund *et al.* 1983). SAM participates in several mammalian methylation reactions, including the methylation of cytosine to from 5-methylcytosine. Alkylating agents can transfer alkyl groups to the nucleophile bases in DNA by attacking the O-and N-positions in base, either through mono- or bifunctional attacks

(Brookes and Lawley 1964;Lindahl 1993;Drabløs *et al.* 2004). Monofunctional alkylating agents have one active group that forms the binding to nucleophilic centres in DNA, while bifunctional alkylating agents have two active groups that can react with two sites on DNA at once results in more complex damages (Drabløs et al. 2004). Among alkylating chemicals are chloroacetaldehyde (CAA) and methyl methanesulfonate (MMS) that cause base damage which may lead to, incorrect base pairing (mutagenic), or blocking of replication (cytotoxic) (Rannug *et al.* 1976;Lundin *et al.* 2005).

1.1.4 Depurination and depyrimidiation

Depurination or depyrimidiation is a major DNA damage is the DNA, where a DNA base is lost and an apurinic/apyrimidinic site (AP-site) is created. AP-site can be formed spontaneously by hydrolysis or as intermediates of base excision repair. Bases are removed from DNA by DNA glycosylase cleavage of N-glycosidic bonds, while the sugar-phosphate chain is kept intact (Friedberg et al. 2006). Depurination occurs with a relatively high frequency. Lindahl and Karlström estimated in 1973 that 2,000 - 10,000 residue in each mammalian cell are depurinated in each generation, while depyrimidiation occurs at a lower rate (Lindahl and Karlstro 1973).

1.1.5 Endogenous DNA damage

DNA in one human cell is estimated to be subject to approximately 20.000 lesions each day due to normal metabolism (Friedberg et al. 2006). The most common damage is the hydrolysis of DNA, with depurination as the most prevalent incident. Other frequent occurring endogenous lesions are generated by oxidation and non-enzymatic methylation of DNA bases (Lindahl and Barnes 2000).

1.2 DNA repair

The first to discover that exogenous compounds could lead to mutations was Hermann Muller in the late 1920s, initiating the research how the cells responded to the different damages (Friedberg 2003). In the years after it, several DNA repair pathways were identified showing high degree of conservation from microorganisms to human cells (Klungland 2001). These repair mechanisms include more than 150 different genes that are involved in different aspects of DNA repair (Wood et al. 2005).

1.2.1 Overview of DNA repair mechanisms

The DNA repair can be divided into six major mechanisms: (i) DNA repair by direct reversal, (ii) base excision repair (BER), (iii) nucleotide excision repair (NER), (iv) nucleotide incision repair (NIR), (v) mismatch repair (MMR), and (vi) double-strand breaks repair (DSBR).

The importance of DNA repair is reflected in the severe diseases and syndromes that appear where there are defects in these repair mechanisms (Thoms et al. 2007).

1.2.2 Direct reversal

Unlike other DNA damage repair pathways, direct reversal is a single-step process that does not include multiple proteins or excision of damaged DNA (Sedgwick *et al.* 2007;Hakem 2008). Direct reversal restores the correct base without removing the damage base, thus no toxic or mutagenic intermediates are generated (Hansen and Kelley 2000). There are several direct repair enzymes reversing different kinds of DNA damage. DNA-photolyase reverses UV-induced thymine dimers by using photons from blue light energy source (Sancar 1990;Todo 1999). Another example of direct reversal is mediated O^6-methylguanine DNA methyltransferase (MGMT) which removes the methyl group of O^6-metghylguanine (Hakem 2008;Hoeijmakers 2009). MGMT performs this important task in a reaction that inactivates the repair enzyme (Mishina et al. 2006). The enzyme being sacrificed for the repair of one single damaged base, and is thus named a "suicide protein" (Liu et al. 2002;Sancar et al. 2004). AlkB is a 2-oxoglutarate- and iron-dependent DNA repair enzyme that releases replication blocks in alkylated DNA by a mechanism involving oxidative demethylation (Falnes *et al.* 2002;Trewick *et al.* 2002;Aas *et al.* 2003). Eight AlkB homologs are identified in human cells (Kurowski et al. 2003): ALKBH2 and ALKBH3 are two human homologs of the *E. coli* AlkB protein, that have shown directly reverse of 1-methyladanine and 3-metylcytosine damage in DNA (Aas et al. 2003;Ringvoll et al. 2006).

1.2.3 Base excision repair

Base excision repair is the major repair pathway for handling endogenous DNA lesions. BER repairs the highest number of DNA lesions in the cells. This can be lesions which, typically consisting of bases modified by relatively small chemical groups, that are induced by ROS, methylation, deamination and hydroxylation (Krokan *et al.* 2004;Dalhus *et al.* 2009). The BER pathway is highly conserved among organisms ranging from *E. coli* to human (Izumi *et al.* 2003;Fortini *et al.* 2003). The repair is initiated by damaging specific enzymes called DNA glycosylases, which recognise and removes the damaged base. DNA glycosylases catalyse the hydrolysis of the glycosylic bond between the base and the sugar of the deoxyribose-phosphate backbone. This leads to release of the damaged base and leaving an AP-site that is both cytotoxic and mutagenic, and requires further processing. The BER pathway may proceed by either "short-patch" (Figure 1.2A and B), involving single nucleotide repair gap, or "long-patch repair" (Figure 1.2C), involving two or more nucleotide repair gaps, after the damage base has been removed by DNA glycosylase and incision has been made by an AP endonuclease (Kubota *et al.* 1996;Klungland and Lindahl 1997). In the short-patch repair the DNA glycosylases only remove the damage base, the gap is filled by DNA polymerase β (Polβ) and DNA ligase III (Lig III) ligates the strand to complete the repair. X-ray repair cross complementing 1 protein (XRCC1) is essential for efficient repair of single strand break repair and stimulates the two last proteins in the pathway (Kubota *et al.* 1996;Brem and Hall 2005). In long-patch repair the strand containing the 5'-deoxyribose phosphatase (dRP) at the incised AP-site is replaced by several nucleotides. The DNA polymerase β, δ and ε synthesize and insert a longer stretch of DNA (2-13 nucleotides) starting at the AP-site (Fortini *et al.* 1998;Stucki *et al.* 1998;Prasad *et al.* 2000). This creates a 5`-flap that is removed by the flap endonuclease 1 (FEN1) (Klungland and Lindahl 1997). The repair is completed by a DNA ligase I (Lig I) which seals the nick. The BER pathway was discovered 36 years ago when it was found that deaminated cytosine (uracil) was released as a free base (Lindahl 1974).

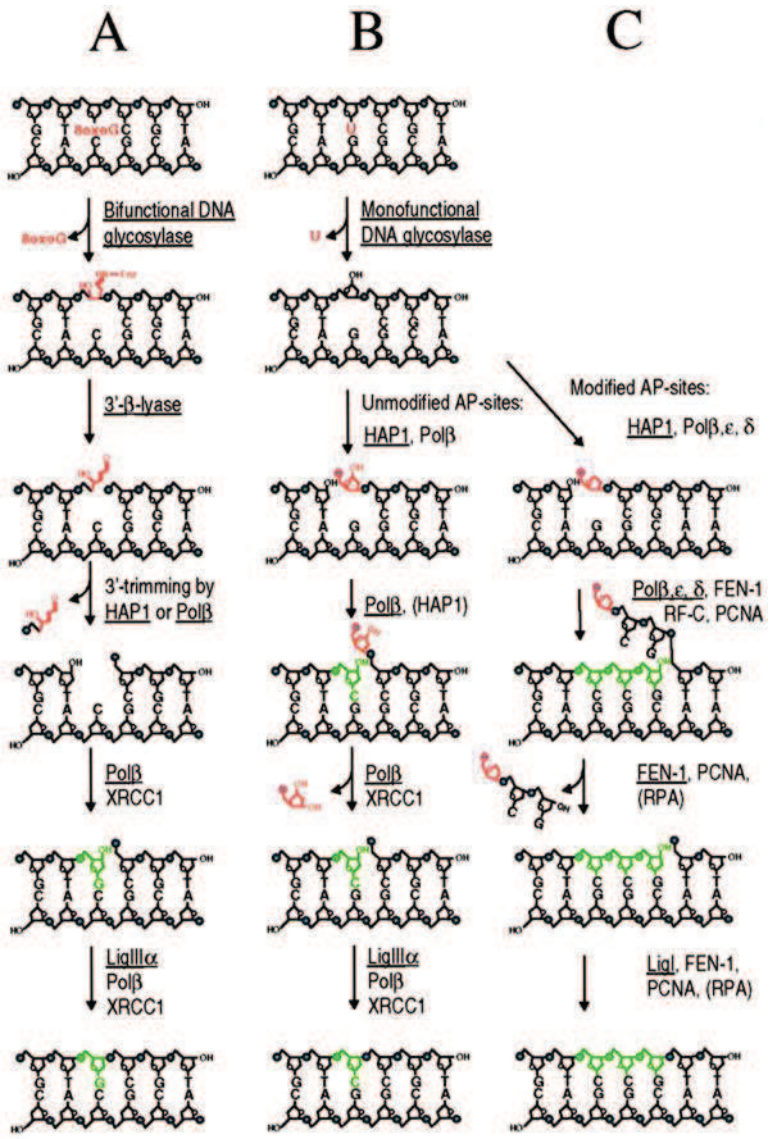

Figure 1.2. The BER pathway is initiated by DNA glycosylases and may follow a short-patch (A and B) or a long-patch (C) route, in part depending on the type of initiating DNA glycosylase. The catalytic protein in each step is underlined (Nilsen and Krokan 2001).

1.2.4 Nucleotide excision repair

Nucleotide excision repair (NER) is one of the most versatile repair mechanisms and can repair many different types of damages (Vermeulen et al. 1997). This pathway is responsible for removal of numerous bulky DNA adducts induced by agents such as UV light and chemicals (polycyclic aromatic hydrocarbons, aromatic amines, and N-nitroso compounds) (Balajee and Bohr 2000). Errors in this repair mechanism can cause serious diseases such as xeroderma pigmentosum, Cockayne's syndrome, and Trichothiodystrophy (Lehmann 2001;Mellon 2005). NER pathway can be divided into two sub pathways: global genome repair (GGR) and transcription coupled repair (TCR). GGR is active in the entire

genome and removes DNA lesions throughout the genome. It is responsible for the repair of the non-transcribed strand of expressed genes and for the repair of unexpressed regions of the genome. TCR ensures quick repair of actively transcribed genes and is specialized to remove damaged DNA from the transcribed strand of transcriptionally active genes (Mellon *et al.* 1987;Christmann *et al.* 2003). NER removes a short stretch of DNA around the damaged region, 12-13 nucleotides in prokaryotic and 24-32 nucleotides in eukaryotic cells. The gap is then filled by DNA polymerases δ, ε or κ, using the complementary strand as template to resynthesize the excised nucleotide sequence, and finally the newly synthesized repair patch is ligated to the pre-existing strand (Vermeulen *et al.* 1997;Reardon and Sancar 2005;Ogi *et al.* 2010). This repair pathway is conserved from prokaryotes to eukaryotes (Seeberg et al. 1976).

1.2.5 Nucleotide incision repair

In 2002, the NIR pathway was first discovered by Ischenko and Saparbaev as a glycosylase-independent incision method of oxdatively damage DNA by *E. coli* endonuclease IV (Nfo) and the homologue *Saccharomyces cerevisiae* Apn1 enzymes (Ischenko and Saparbaev 2002). The NIR pathway is initiated when an AP endonucleases, incise DNA 5' to a number of oxidatively damaged bases. The AP endonuclease leaves the lesion attached to the 5' end of the downstream fragment and on OH-group on the 3'end of the nicked site. NIR has an advantage over BER: does not form AP sites, and thereby avoids the genotoxic intermediates like BER (Gros et al. 2004). Gros and co-workers reported that Ape1 is the major AP endonucleases in human cells, and there was specific endonuclease damage in the NIR Pathway (Gros et al. 2004). The NIR pathway is conserved from *E. coli* to humans (Ishchenko *et al.* 2003;Gros *et al.* 2004). Downstream steps in NIR pathway is poorly described and it is suggested that NIR merged with long-patch BER (Ischenko and Saparbaev 2002).

1.2.6 DNA mismatch repair

DNA mismatch repair (MMR) is a system for eliminating base-base mismatch and insertion/deletion loops, which have been introduced by replication misincorporation and slippage (Hoeijmakers 2001;Christmann *et al.* 2003). MMR repair strategy is an integrated part of DNA replication (Friedberg et al. 2006) and is highly conserved from *E. coli* to mammals (Li 2008). In bacteria, yeast and higher eukaryotes, different types of MMR exits, still the general MMR process have many similarities (Fishel and Kolodner 1995). The MMR repair machinery must distinguish between the "correct" and "mismatched" DNA strand in order not to introduce a mutation (Yang 2000;Christmann *et al.* 2003). Mutations in MMR

genes are associated with an increase in the frequency of spontaneous mutation a contributing factor to hereditary nonpolyposis colorectal cancer (HNPCC) (Leach *et al.* 1993;Fishel *et al.* 1994). MMR is also involved in cell cycle arrest and apoptosis (Li 2008).

MMR is strand-specific, and as for most other DNA repair pathways is well characterized in *E. coli*. MutS initiates MMR by recognizing mismatches in DNA. Then MutL and MutH are recruited. This protein complex activates a methylation-specific endonuclease activity of MutH, which nicks the newly synthesized DNA strand at hemi-methylated GATC site near the mismatch (Nowosielska and Marinus 2008). DNA helicase II then separates the two strands and exonuclease excises the DNA from the nick past the mismatch (Dao and Modrich 1998). The DNA polymerase δ and coats ssDNA fills in the gap and DNA ligase seals the strand (Lahue *et al.* 1989;Kunkel and Erie 2005).

Eukaryotes have a similar mechanism for MMR, but are more complicated because of several MutS- and MutL- homologous proteins. The details of MMR in the eukaryotic pathway is not fully understood, but the damage excision and strands synthesis is carried out by Exonuclease I (ExoI), replication protein A (RPA), proliferating cellular nuclear antigen (PCNA), DNA polymerase δ, and DNA ligase I (Li 2008).

1.2.7 Double-strand breaks repair

Recombination repair is fundamental cellular process in all living organisms; it is responsible for correction of double-strand breaks (DSBs). DSBs must be efficiently repaired to restore the integrity and functionality of the genome. If the cell does not repair this damage it can be lethal (Cahill et al. 2006). These DSBs may occur as a result of ROS, ionizing radiation, various chemicals or due to collapsed replication fork (Karran 2000).

The DSBs repair pathway can be divided into two main repair pathways, non-homologous DNA end-joining (NHEJ) and homologous recombination (HR). Both mechanisms are evolutionarily conserved (Lee and McKinnon 2007). Depending on the position in the cell cycle, one of the two repair mechanisms is activated, or both pathways may be activated to simultaneously and cooperatively repair DNA lesion (Moore and Haber 1996). NHEJ is most active in G0/G1, whereas HR occurs mostly in late S and G2 phase (Christmann et al. 2003). Although the two repair mechanisms are different and involve many different enzymes, both require kinase ATM to signal failure and locate the damage. One other area that is different is that NHEJ which leads to an increase or loss of a few nucleotides, while HR is an error-free repair mechanism (Slupphaug et al. 2003).

1.2.7.1 Homologous recombination

After a double strand breaks, a complex of exonucleases consisting of Mre11/Rad50/NBS1 (M/R/N) will remove additional nucleotides in 5' → 3' direction form one of the damage strands, causing single-strand ends, as shown in Figure 1.3A. Rad52 in eukaryotes and RecA in prokaryotes binds to the 3' single-strand tails and ensure that RAD51, along with several proteins, will help to find the homologous sequence in the sister chromatids (Slupphaug et al. 2003). Initiating a strand invasion followed by branch migration leads to the formation of the Holliday junction, which in turn degrades the resolvases such as RuvC. The ligase will eventually glue the ends of the recombinant DNA molecule.

HR mechanism can also follow a different repair pathway that do not results in Holliday junction, but rather leads to single-strand annealing (SSA). The M/R/N-complex will continue to remove nucleotides in the 5' → 3' direction until the homologous end. RAD52 or RecA would then ensure that the homologous sequences are matched so that the strands can be ligated. This repair pathway will, in contrast to the "regular" HR repair, lead to loss of some parts of the sequence (Sancar et al. 2004).

Homologous recombination (HR) is involved in DSB repair damaged, replication-fork rescue, segregation of homologous in meiosis, and telomere maintenance (Sung and Klein 2006). Although only 10 % of DSBs are repaired by this pathway in mammals, defects in the HR machinery can lead to serious medical disorders like the human syndromes AT-like disorder (ATLD) and Nijmegen breakage syndrome (NBS) (Thompson and Schild 2002;Hakem 2008).

1.2.7.2 Non-homologous end-joining

NHEJ is initiated when the proteins KU70 and KU80, which serves as a heterodimer, binds to DNA ends. The proteins then recruit the regulatory subunit, DNA-PKCS, so it can also bind to the KU-proteins. The M/R/N-complex helps to recruit XRCC4 forming a complex with ligase IV which links the DNA ends together, see Figure 1.3B (Sancar et al. 2004).

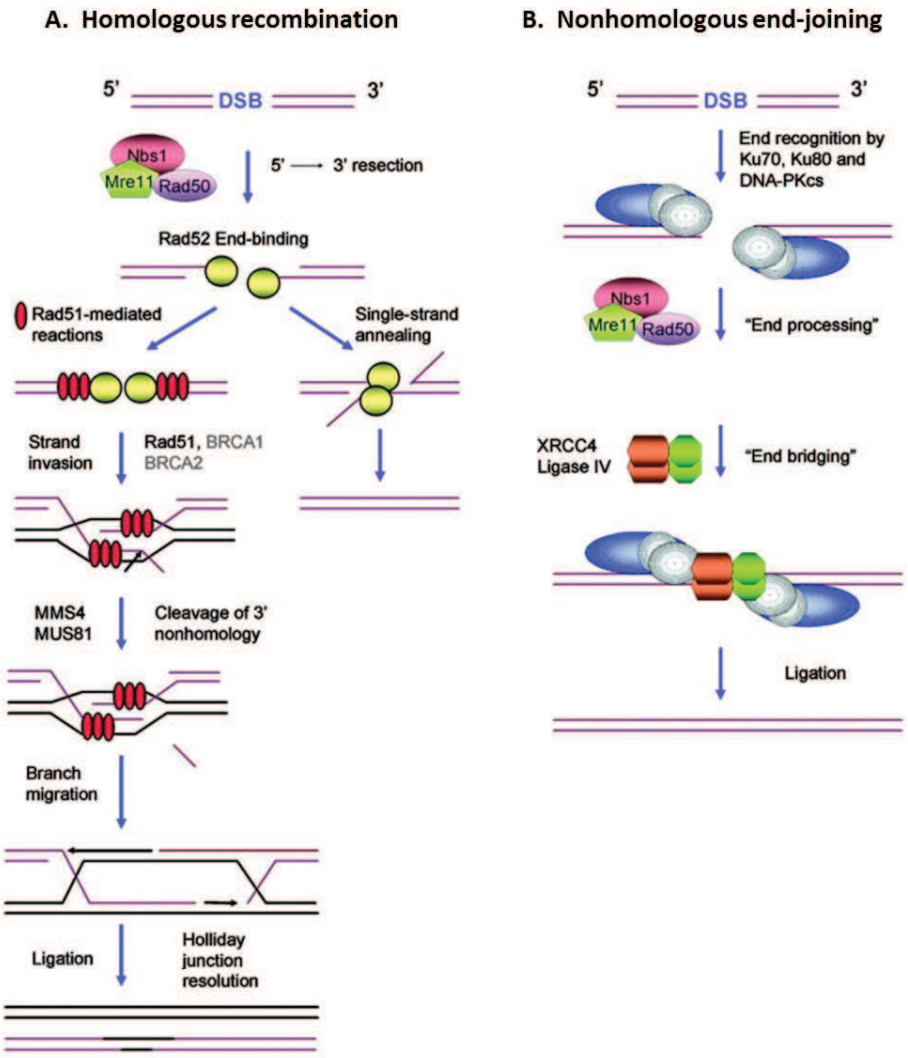

Figure 1.3. Homologous recombination and non-homologous end-joining. A) The illustration shows the way of repairing a double-strand breaks, which either leads to a Holliday junction or a single-strand annealing. B) Schematic representation of non-homologous end-joining (Sancar et al. 2004).

1.3 Endonuclease V

Endonuclease V (EndoV) belongs to a large group of homologous proteins, conserved from prokaryotes to human (see Appendix III for multiple sequence alignment). In prokaryotes, EndoV has a specific affinity for deaminated DNA bases, and initiates nucleotide incision repair (NIR). The role of EndoV in higher organisms is less known, but the data obtained from studies of EndoV in simple organisms provides a starting point for examination of mammalian and specifically human ENDOV, which has been the topic of this master thesis.

1.3.1 Prokaryotic EndoV

1.3.1.1 Endonuclease V from *Escherichia coli*

E. coli EndoV (EcEndoV) is the main repair enzyme of deaminated bases in *E. coli* cells (Weiss 2008). The gene that is encoding for EndoV, *nfi (endonuclease five)*, was characterized by Gates and Linn in 1977, where they found that the enzyme had substrate specificity for uracil in DNA (Gates and Linn 1977;Guo et al. 1997). EcEndoV's main substrate is deaminated adenine, hypoxanthine, but the enzyme also recognizes other deamination products like xanthine and uracil. It is known that EcEndoV recognizes abasic site, urea residues, hairpins, unpaired loops, tetrahydrofuran (THF), different types of flaps, and pseudo-Y DNA structures (Yao *et al.* 1994;Yao and Kow 1996;Yao and Wah-Kow 1997;He *et al.* 2000). The protein initiates repair by creating a nick at the second phosphodiester bond at the 3' lesion, that will result in 3'-hydroxyl and 5'-phosphoryl groups (Guo et al. 1997).The nick will not remove the damage DNA, so proteins have to complete the repair pathway. No known proteins have been identified or characterized, however it is assumed that the EndoV incision is followed by an exonuclease, polymerase, and ligase activity (He et al. 2000). Figure 1.4 shows the suggested pathway for deaminated purines.

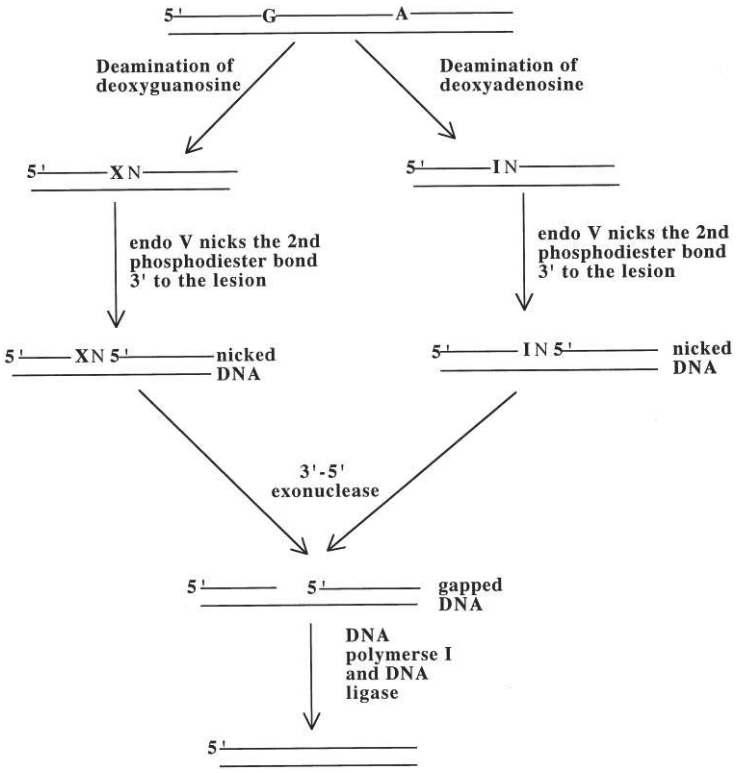

Figure 1.4. Scheme for the proposed repair pathway of deaminated purine in *E. coli* (He et al. 2000). EndoV nicks the second phosphodiester bond 3' to the deaminated deoxyguanosine (xanthine, X) or deaminated deoxyadenosine (inosine, I) lesion. The nicked DNA is processed by an unknown 3`-5` exonuclease, creating a single-stranded gap. DNA polymerase I synthesises the correct piece of DNA and ligase ligates the DNA. N = general nucleotide.

The affinity to hypoxanthine lesions for EndoV is 20 times higher than mismatches, and EndoV cleaves both single-stranded and double-stranded hypoxanthine-containing DNA (Yao and Wah-Kow 1997). It has been shown that the enzyme specificity towards mismatches are reduced if G:C or C:G base pairs are located close to the lesion. The specificity towards hypoxanthine is not affected by this, implying that Endo V has different binding interactions with DNA depending on which lesion is present (Yao and Wah-Kow 1997;Kow 2002).

1.3.1.2 Endonuclease V from *Thermotoga maritima*

Thermotoga maritima EndoV (TmaEndoV) has been found to have the same endonucleolytic activity of deaminated DNA bases as EcEndoV. Both TmaEndoV and EcEndoV require a metal ion (Mg^{2+} or Ca^{2+}) to reach optimal affinity for inosine. There has been suggested that the 6-keto group in inosine and xanthine, and the 4-keto group in uracil interact with the protein which may create a local distortion in the DNA helix which can help recruit EndoV (Huang et al. 2001). Structural studies of TmaEndoV in complex with a hypoxanthine-containing DNA duplex revealed the molecular details of the interaction between the protein and the DNA. TmaEndoV is a αβα globular protein with an RNase H-like motif also found in *E. coli* RNase H (Dalhus et al. 2009). Dalhus et al. have shown the mechanism for how TmaEndoV initiates the repair of hypoxanthine in DNA. TmaEndoV contains a damage recognition "pocket" that can distinguish between undamaged and damaged bases. The enzyme also has a well-conserved sequence motif, PYIP (Pro79-Tyr80-Ile81-Pro82). PYIP motif separates the two DNA strands and pushes the residue on the complementary strand partially out of the protein-DNA complex. The hypoxanthine base is rotated around 90° between the side chains of Leu85 and Leu142 (Dalhus et al. 2009).

1.3.2 Eukaryotic EndoV

EndoV was first discovered and characterized in prokaryotes, but the search for homologues in eukaryotes started early. Yao and Kow came with the hypothesis that the yeast RTH1 nuclease and the human and murine FEN1 might be the EndoV functional homologues in *Saccharomyces cerevisiae* (Yao and Kow 1996). EndoV was later characterized as a highly conserved protein in higher organisms (Aravind et al. 1999;Feng et al. 2005).

1.3.2.1 Endonuclease V from *Mus musculus*

Moe and her co-workers started with a search in the database for expressed sequence tags (ESTs) using *EcEndoV* as query, from this search *Mus musculus EndoV* (*mEndoV*) was identified (Moe et al. 2003). This study showed that mEndoV had a weak endonuclease activity of hypoxanthine in the DNA. The activity of mEndoV towards double-stranded substrate was higher than for the single-stranded substrate, but no other robust enzyme activities have been found so far. Mouse cDNA from *EndoV* is cloned in *E. coli* cells and found to be expressed in various tissues (Moe et al. 2003).

1.3.2.2 Endonuclease V from *Homo sapiens*

The gene for human Endonuclease V (*hENDOV*) is found in the human EST database by Moe et al. (Moe et al. 2003). From this human EST database many different isoforms of the protein were found, probably representing incomplete and uncorrected sequences from high-throughput DNA sequencing.

1.4 Mouse as a model organism

Model organisms are widely used for the different opportunity to mutate individual genes and study the effects. This can be done either by site specific gene-targeting or by random mutagenesis. For random mutagenesis, subsequent identification of the targeted allele is required. One of the original models for molecular biology was the bacterium *E .coli,* while several bacterial viruses (bacteriophages such as Lambda and T4) have been vital for the study of gene structure and regulation (Fields and Johnston 2005).

In eukaryotes, a number of yeast species, particularly *S. cerevisiae,* have been extensively studied in genetics and cell biology, mainly because they are quick and easy to grow. The fruit fly *Drosophila melanogaster* is commonly used, due to its rapid life cycle, and various visible hereditary traits (Fitzgerald-Hayes and Reichsman 2010). The roundworm *Caenorhabditis elegans* has defined development patterns, and can quickly be examined for abnormalities (Fields and Johnston 2005). The list of model organism also includes plant (*Arabidopsis thaliana*) and fish (zebrafish; *Brachydanio rerio*).

The household mouse (*Mus musculus)* had been used as a model organism for nearly 35 years and numerous experiments have been conducted with this small mammal. These experiments have contributed significantly to our knowledge of mammalian biology, development and pathology. The mouse and human genomes mouse models have approximately the same size, contain the same number of genes and show extensive synteny (conserved gene order) (Pennacchio 2003). Mutations that cause diseases in humans often cause similar diseases in mice. Importantly, mice have genes that are not represented in other animal models (the fruit fly and roundworm), including the genes of the immune system (Alberts et al. 2008). A principal strategy employed by scientists today is to convert analytical data from DNA sequence information into knowledge about functional processes. Functional analysis of mammalian gene *in vivo* is primarily achieved by the analysis of knockout mice (Chan et al. 2007). Considerable information about genes involved in the regulation of embryo development and pathophysiology has emerged from the use of transgenic technology over recent years.

The deletion of a gene in a mouse is referred to as a knockout mouse. A knockout mouse deficient in a particular gene – the gene of interest – is created by the introduction of a deletion-construct into embryonic stem (ES) cells *in vitro*. The deletion construct is able to integrate into the ES cell genome by homologous recombination. The ES cells that contain the deletion-construct in the genome are microinjected into host blastocysts to produce ES cell-mouse chimeras, which are recognizable by their variegated coat colour at birth. Chimeras are bred to obtain offspring with the deletion introduced into the germline.

The knockout mice may not have any obvious phenotype, which might be due to genetic redundancy, nature of the knockout alleles, or genetic background effects. For other genes, the mutants die *in utero* owing to the critical roles of these genes in embryonic development (Chan et al. 2007). To overcome embryonic lethality and obtain more precisely controlled gene expression in a spatiotemporal manner, conditional knockout approaches have been developed (Bockamp et al. 2002).

1.5 Aim of the study

Prokaryotic EndoV has been shown to bind to and initiate repair of different DNA lesions, through the nucleotide incision pathway. The protein is an endonuclease, and is most effective on its main substrate hypoxanthine. An RNase H-like motif similar to a motif in the Holliday junction resolvase RuvC has been identified as an important part of EndoV, and it can thus be speculated if EndoV has a role in genetic recombination. The ENDOV homologue in human has been identified, and has high sequence conservation with the prokaryotic forms. However, no characterisation of human Endonuclease V is published. Since all key residues responsible for DNA binding and catalysis in prokaryotic EndoV seem to be conserved, a study of hENDOV would be of great interest.

Recently, several isoforms of hENDOV have been experimentally confirmed in our laboratory by the sequencing of a human fibroblast cDNA library. The exon boundaries have been found, and some isoforms were selected as the most probable representative forms of hENDOV. NCBI Reference Sequence (RefSeq) annotates three representative transcripts the Homo sapiens locus FLJ35220, encoding *hENDOV*: NM_173627.3, NM_001164637.1 and NM_001164638.1.

The aim of the study was to characterize the Endonuclease V from human (*Homo sapiens*) and mouse (*Mus musculus*). Since several isoforms of hENDOV exist, we wanted to look at the expression of the different transcripts variants of *hENDOV* in the human cells. Furthermore, we wanted to study the intracellular localization of hENDOV by GFP-fusion protein analysis. Together with Professor A. Klungland and his group at the same department, we wanted to study the phenotype of mice in which the *mEndoV* gene has been knocked out. This knocked out mouse already exists in the laboratory.

2 Materials

2.1 Reagents

2.1.1 Chemicals

Chemicals	Supplier
Acetic acid	MERCK
Bacto Agar	Difco
Bacto-tryptone	Difco
Bacto yeast extract	Difco
BioRad Protein Assay	BioRad
Boric acid	MERCK
Bovine Serum Albumin (BSA)	BioLabs® Inc.
Difco Luria Bertani (LB)-Broth	Difco
Dimethyl sulfoxide (DMSO)	Sigma Aldrich
Dithiotheritol (DTT)	Sigma Aldrich
DNA Loading Dye Solution (6x)	Fermentas
dNTP Mix, AB-0196	Pharmacia
Dulbecco`s Modified Eagle Medium with 4.5 g/l Glucose (DMEM)	Lonza BioWhittaker
Ethanol 100%	Kemityl
Ethylenediaminetetraacetic acid (EDTA)	Sigma Aldrich
Fetal Bovine Serum (FBS)	PAA Laboratories GmbH
GlutaMAX™	Gibco
Glycerol	Sigma Aldrich
Glycine	MERCK
Hydrochloric acid fuming 37% (HCl)	MERCK
IPEGAL® CA-630	Sigma Aldrich
Isopropanol	MERCK
Kanamycin	Sigma Aldrich
Magnesium chloride ($MgCl_2$)	MERCK
Methanol	VWR
Methyl methane sulfonate (MMS)	Sigma Aldrich
MTT, 3-[4, 5-dimethylthiazol-2-yl]-2, 5-diphenyl tetrazolium bromide	Sigma Aldrich
NuPAGE® LDS Sample Buffer 4x	Life Technologies
NuPAGE® MOPS SDS Running Buffer 20x	Life Technologies
Penicillin-streptomycin (Pen-Strep)	Lonza BioWhittaker
Phenylmethylsulfonyl fluoride (PMSF)	Sigma Aldrich
Phosphate buffered saline (PBS) Buffer 10x	Sigma Aldrich
Potassium chloride (KCl)	MERCK

Chemicals	Supplier
Protease Inhibitor Cocktail, P8340	Sigma Aldrich
Skim milk Powder	Fluka
Sodium chloride (NaCl)	Sigma Aldrich
Sodium Deoxy cholate (DOC)	Sigma Aldrich
Sodium dodecyl sulphate (SDS)	Sigma Aldrich
Sodium hydroxide (NaOH)	MERCK
SYBR® Safe DNA gel stain	Life Technologies
Tris Base	Sigma Aldrich
Tris-HCl (pH 8.0)	Sigma Aldrich
Triton X-100	Sigma Aldrich
Trypan Blue Stain	Life Technologies
Trypsin-EDTA	Lonza BioWhittaker
Tween®20	Sigma Aldrich
UltraPure™ Agarose	Life Technologies

2.2 Biological materials

2.2.1 Bacterial strains

Strain	Characterstics	Genotype	Reference
ER2566	*E. coli*	F⁻ *λ- fhuA2 [lon] ompT lacZ::T7 gene 1 gal sulA11 Δ(mcrC-mrr)114::IS10*	New England Biolabs
DH5α™-T1^R	*E. coli*	F- *φ80lacZΔM15 Δ(lacZYA-argF)U169 recA1 endA1 hsdR17(rk-, mk+) phoA supE44 thi-1 gyrA96 relA1 tonA*	Life Technologies

2.2.2 Cell types

Cell type	Description	Reference
HeLa-S3	Human cervical carcinoma	ATCC
HaCaT	Human immortalized keratinocytes	ATCC
Early transformed MEF WT	Mouse embryonic fibroblast, *mEndoV* +/+	From our laboratory
Early transformed MEF KO	Mouse embryonic fibroblast, *mEndoV* -/-	From our laboratory
Primary MEF WT	Mouse embryonic fibroblast, *mEndoV* +/+	From our laboratory
Primary MEF KO	Mouse embryonic fibroblast, *mEndoV* -/-	From our laboratory

2.2.3 Plasmids

Plasmid	Characteristics	Reference
pEGFP-N1	N-terminal EGFP-tag	Clontech
pEGFP-C1	C-terminal EGFP-tag	Clontech
pEGFP-transcript 1	*hENDOV* with exon3 and short exon9 +exon10	This study
pEGFP-transcript 2	*hENDOV* without exon3 and with short exon9 + exon10	This study
pEGFP-transcript 3	*hENDOV* without exon3 and with full length exon9	This study

2.2.4 Antibodies

Antibody	Host	Dilution	Manufacturer
Anti-hEndo V, PP132	Rabbit	1:1000	Eurogentec
Anti-hEndo V, GP132	Rabbit	1:1000	Eurogentec
Anti-hEndo V, SAB132	Rabbit	1:1000	Eurogentec
Anti-hEndo V, GP133	Rabbit	1:1000	Eurogentec
Anti-hEndo V, SAB133	Rabbit	1:1000	Eurogentec
Anti-GFP (B-2): sc-9996	Mouse	1:1000	Santa Cruz Biotechnology
Anti-FLJ35220, ab69400	Mouse	1:1000	Abcam
Fibrillarin antibody, ab4566	Mouse	1:100	Abcam
Rabbit anti-Goat IgG H&L (Biotin), ab 6740	Rabbit	1:20 000	Abcam
Goat anti-mouse antibody conjugated to HRP, 115-036-068	Mouse	1:30 000	Jackson ImmunoResearch
Alexa Fluor® 594 Goat Anti-Mouse IgG (H+L), A11005	Mouse	1: 1000	Life Technologies
Protein A/G PLUS-Agarose: sc-2003	-	-	Santa Cruz Biotechnology

2.2.5 Enzymes and buffers

Enzyme	Supplier
EcoRI	New England Biolabs
NEBuffer *EcoRI* (10x)	New England Biolabs
AmpliTaq Gold® DNA Polymerase	Applied Biosystems
Reaction 10x buffer II	Applied Biosystems

2.2.6 Primers

"f" (forward) and "r" (reverse).

Primer ID	Sequence 5'→ 3'	Description
650	TAATACGACTCACTATAGG	T7 promotor
4890	CAGGAAACAGCTATGA	M13 (r)
4891	GTAAAACGACGGCCAG	M13 (f)
13253	CCTTCTTGTGGATGGAAACGGGGTAC	GSP2 (f)
13254	GTCGTGGCTCCTCAGGGCCATTC	GSP1 (r)
AP1	CCATCCTAATACGACTCACTATAGGGC	Adaptor primer 1
AP2	ACTCACTATAGGGCTCGAGCGGC	Adaptor primer 2
13708	GCCACCTTGGCGTCCTTACAGACC	Nested primer 2 (f)
13709	CTCCCAGCAGAGGGAATGAGTCTCC	Nested primer 1 (r)
13735	GTGCTTCCCTGGTGGTGC	exon3 (f)
13737	GCCAGGAAGCCCGACACGTAGG	exon3 (r)
13738	TCGGGGGCGTTGACGTG	Δexon3 (f)
13739	CCACAAGAAGGACCTCGAG	Δexon3 (r)
13740	GCATGCCCCAAAGGAGACT	Full length exon9 (f)
13741	TGCTCCTGGGAGCCTGG	Full length exon9 (r)
13742	CAAGTCGCTGGGACTCCC	short exon9 + exon10 (f)
13743	TCAACAAAGTGCTGAGGACTC	short exon9 + exon10 (r)

2.3 Other materials

2.3.1 Molecular Markers

Standard	Manufacturer
SeeBlue® Plus2 Pre-Stained Standard	Life Technologies
GeneRuler™ DNA Ladder Mix	Thermo Scientific

2.3.2 Kits

Kit	Manufacturer
Qiagen Plasmid Midi Kit	Qiagen
Qiagen Plasmid Mini Kit	Qiagen
Immun-Star™ WesternC™ Kit	BioRad
TOPO® TA Cloning® Kit with One Shot® MAX Efficiency™ DH5α-T1R *E. coli*	Life Technologies
FuGENE® 6 Transfection Reagent	Roche

2.4 Equipment and instruments

2.4.1 Technical equipment

Device	Model	Supplier
Centrifuge	Allegra™ X-22 Centrifuge	Bechman Coulter
	Spectrafuge mini	Labnet
	Spectrafuge maxi	Hitachi
	Magefuge	Heraeus
Spectrophotometer	UV-visible spectrophotometer UV-160 I	Shimadzu
	NanoDrop ND-1000	Thermo Scientific
	Wallac Victor^2 1420 multilabel counter	Wallac
Incubator	Innova 400 incubator shaker	New Brunswic scientific
	Innova 4300 incubator shaker	New Brunswic scientific
	Termaks incubator	Termaks
	Forma Steri-cycle CO_2	Thermo Scientific
	Waterbath	KeboLab AS
Power supply	Electrophoresis constant	Amersham Biosciences
	Power supply EPS 60	Pharmacia biotech.
	Power supply ECPS 3000/150s	Pharmacia biotech.
PCR machine	PTC-200 Peltier Therrmal Cycler	MJ research
Sterile hood	Holten Lamin air	Holten
Imager	Alphamager	Alpha Innotech
	BioRad Molecular Imager PhosphorImager	BioRad
Sequencing machine	3730 DNA Analyzer (48 capilary)	Hitachi
Confocal microscopy	LSM 510	Carl Zeiss
Sonicator	LabSonic™ M	Sartorius Stedim Biotech
Weighing scale	AT261 Delta Range	Amersham Biosciences
	BR 4100	Amersham Biosciences
Various	Countess™ Automated Cell Counter	Life Technologies
	Countess™ cell counting chamber slide	Life Technologies
	iBlot® Gel Transfer Device	Life Technologies
	iBlot® Transfer Stack, PVDF Regular	Life Technologies
	NuPAGE® 12 % Bis-Tris-gel	Life Technologies
	Nuclon™ T-25, T-75, and T-175 cm^2, filter cap	Thermo Scientific

2.4.2 Software

Software	Source
Image Lab	BioRad
Wallac 1420 Manager	Wallac
NCBI Blast	NCBI
Zeiss AIM 4.2	Carl Zeiss
Zeiss LMS Image Browser	Carl Zeiss

2.5 Recipes

2.5.1 Solutions and buffers

Solution and buffers	Compostion
RIPA lysis buffer	150 mM NaCl 1 % IPEGAL® CA-630 0.5 % DOC 0.1 % SDS 1 mM PMSF
2x Sample buffer	2x NuPAGE® LDS Sample buffer 20 mM DTT
PBS-T	1xPBS 0.05 % Tween®
Blocking buffer	5 % Skim Milk Powder in 1xPBS
1xTBE	90 mM Tris base 90 mM Boric acid 2 mM EDTA (pH 8.0)
1 % Agarose	0.5 g Agarose 50 ml 0.5 x TBE 1.5 µl SYBR Safe
MTT solution	5 mg/ml MTT in 1xPBS
Solubilization solution	10 % SDS in 0.01 M HCl

3 Methods

3.1 General methods used for molecular biology

3.1.1 Miniprep and Maxiprep for plasmid purification

Isolation of plasmid DNA was done with Qiagen® Plasmid Mini kit and Midi kit. The method is based on the use of anion exchange columns where the column material containing diethylaminoethanol binds to the negatively charged phosphates of DNA. Impurities such as RNA and proteins are removed with a buffer. (Qiagen® 2005).

The procedure was taken from Qiagen® Plasmid Purification Handbook, November 2005, third edition.

3.1.2 Subcloning

The DNA was digested with *EcoRI* enzyme to verify the subcloning procedure (Section 3.2.1) and separated on 1 % (w/v) TBE-agarose gel. The DNA fragments of interest were purified using QIAEX II gel extraction kit (Qiagen) following the manufacturer's instructions. Concentrations were measured with NanoDrop ND-1000 Spectrophotometer (Thermo Scientific).

3.2 5'RACE and 3'RACE experiments

Marathon-Ready™ cDNAs (Clontech) are tissue-specific pools of cDNA ready for use in 5'RACE and 3'RACE PCR. Each Marathon-Ready™ cDNA is synthesized from high-quality Premium Poly A^+ RNA and ligated to the Marathon Adaptor. A sets of gene-specific 5' and 3' ends primers against *hENDOV* and adaptor primer 1 (AP1) were used to amplify a RACE products from cDNA pool from human brain (Clontech). After sequencing of the RACE products, a complete full-length cDNA clone can be obtained by end-to-end PCR.

The standard PCR program and reaction concentrations used is listed below in Table 3.1. If more than one PCR-reaction was made, a master mix containing the polymerase, dNTP, PCR-buffer and water was made giving more precise concentrations in the mix.

Table 3.1 Standard PCR program with AmpliTaq Gold® DNA Polymerase.
*Annealing temperatures should be chosen to match the Tm values of the primer pair.

2.5 µl	10x buffer II
2.0 µl	dNTP
3.0 µl	MgCl2 (25 mM)
1.0 µl	Primer Fv (10 µM)
1.0 µl	Primer Rv (10 µM)
0.3 µl	AmpliTaq Gold® DNA Polymerase
5.0 µl	cDNA
10.2 µl	MQ H2O
25 µl	Total volum

T [ºC]	Time		
95	9	min	
95	30	sec	Repeat 30 times
65*	30	sec	
72	1	min	
72	5	min	
4	Hold		

3.2.1 TOPO-TA cloning

The 3.9 kb pCR®2.1 cloning vector following the **TOPO® TA Cloning® Kits** (Life Technologies) were used to subclone the RACE products of Marathon-Ready™ cDNA from brain for validation by sequencing. The plasmid is linearized and contains cohesive 5' ends (Figure 3.1) with a thymidine overhang allowing for easy insertion of PCR fragments amplified with AmpliTaq Gold® polymerase, which leave adenine overhangs on amplified fragments. A blunt end DNA fragment that does not contain adenine overhangs can be incubated with AmpliTaq Gold® polymerase for addition of these. The fragment with adenine overhangs should be used for TOPO-TA cloning within 24 hours as the 3' overhangs degenerate. The ligation into this backbone and transformation into competent *E. coli* is carried out as described in the manufacturer's instructions. The DNA sequencing was carried in our own sequencing department.

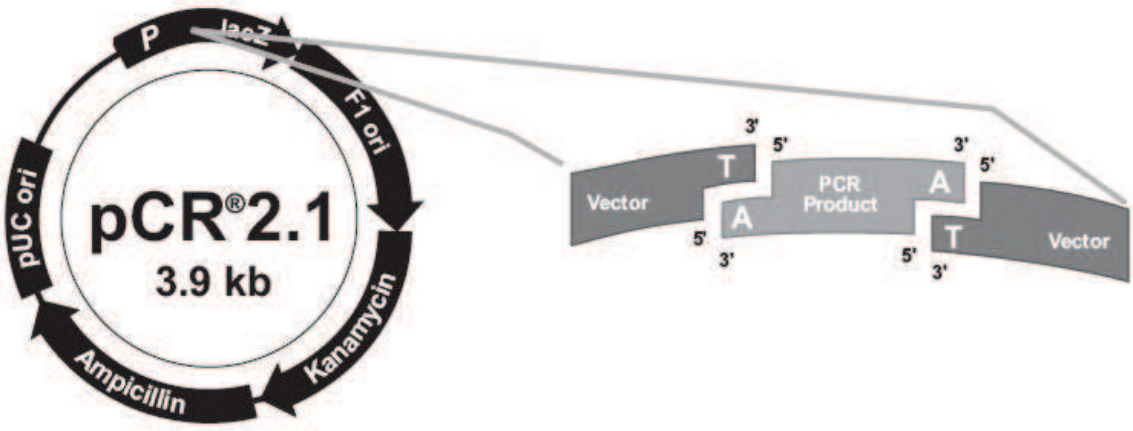

Figure 3.1 Linearized TOPO-TA cloning vector for insertion of fragments with adenine overhang.

3.3 Standard cell culture procedures

3.3.1 Subculture and maintenance of cell lines

To prevent contamination, cell culture work was performed in laminar air flow hoods (LAF-hood) using sterile techniques. The cell lines were grown in DMEM/F-12 medium containing L-glutamine (Lonza BioWhittaker). Additional supplements of fetal calf serum (PAA) (respectively, 10 % for the HeLa-S3 and HaCaT, and 15 % for the early transformed and primary MEF *mEndoV* +/+ and *mEndoV* -/- cell lines), 100 U/ml penicillin and 100 U/ml streptomycin (Penicillin-Streptomycin solution, Lonza BioWhittaker), and 1x GlutaMAX™-I (Gibco) were added to make complete growth medium (this composition will from now on be referred to as "medium"). The cells were grown in sterile Nunclon flasks with filter caps, T-25, T-75, and T- 175 (cm^2 of surface area) and incubated at 37ºC in humid atmosphere with 5% CO_2, from now on referred to as "incubation".

3.3.2 Subculture of adherent cell lines

Procedure:

1. The cell medium was removed from the primary culture and washed with 5 ml 37°C 1xPBS to remove any residual fetal calf serum which may inhibit the action of trypsin.
2. 1 ml preheated trypsin-EDTA (Lonza BioWhittaker) was added to the culture flask and incubated for about 5 minutes.
3. The cell culture was monitored under a light microscope to visualize the detachment process.
4. 9 ml fresh medium was added to the culture to neutralize the trypsin-EDTA. The cell suspension was flushed against the flask bottom until all cell clumps were dispersed and loosely attached cells were detached.
5. A fraction of the cell suspension was transferred to a new culture flask containing different amounts of fresh medium. The total amount in each T-75 culture flask was 18 ml. The subcultivation ratio was 1:10 and 1:20 for HeLa-S3 and HaCaT cell line and 1:10 for MEF cell lines.

3.3.3 Viable cell quantification

Before every experiment, the cells were detached from the culture flask by trypsin-EDTA and counted to ensure reproducibility. A small volume of the mixed cell suspension was counted to find the correct cell number. Cell counting was performed visually by using The Countess® Automated Cell Counter (Life Tecnoloiges).

Procedure: 10 µl of the cell sample is mixed with 10 µl supplied trypan blue and loaded to a Countess™ cell counting chamber slide. The camera acquires cell images from the sample on the slide and the image analysis software automatically analyzes acquired cell images, and measures cell count and viability using the trypan blue stain.

3.3.4 Transient transfection of HeLa-S3 cell line

The cells were transfected with the plasmids: pEGFP-N1, pEGFP-transcript 1, pEGFP-transcript 2, and pEGFP-transcript 3 (Section 2.2.3). The following protocol is for 10 cm dish (medium: 10 ml).

Procedure:

1. FuGENE6 (Roche) was added to the cells in a 3:1 ratio to DNA (10 µg DNA with 30 µl FuGENE6 for 100 mm dishes).
    a. The FuGENE6 was diluted in serum free medium (30 µl FuGENE6 in 70 µl medium for each transfection) mixed gently and incubated for 5 min at room temperature (RT).
    b. 10 µg DNA was added to the FuGENE6/medium and the tube was flicked and incubated for 15-20 min at RT.
    c. The transfection reagent was added to the cells in a drop-wise manner to ensure distribution over the entire plate surface.
2. The cells were harvested 24 hour after the transfection.

3.4 Immunoprecipitation (IP) of hENDOV

Analyses of target proteins can be done by specifically purification with corresponding antibody

3.4.1 Preparation of cell lysates

Procedure:

1. The cells were harvested cells from four 80 % confluent T-175 flasks of HeLa-S3 and HaCaT.
2. The HeLa-S3, HaCaT, and transient transfected HeLa-S3 (Section 3.3.4) cells were washed once with ice-cold 1xPBS and spun down at 2000 g, for 5 minutes.
3. 1 ml of ice-cold RIPA lysis buffer (150 mM NaCl, 50 mM Tris pH 8.0, 1% IPEGAL® CA-630, 0.5% DOC, 0.1 % SDS, 1 mM PMSF, and 1 mM protease inhibitor cocktail, P830 (Sigma Aldrich)) were added to the cell pellets.
4. The cells were sonicated on ice for 2x20 sec.
5. All the samples were then spun down at 12.000 g, 4°C, for 10 minutes. The supernatants were transferred to fresh tubes and snap frozen in nitrogen. All the cell lysates were stored at -80°C until needed.

3.4.1.1 Determination of protein concentration

The protein concentrations from all cell lysate were the measured by Bradford Protein Assay (Bio-Rad) using a UV-visible Spectrophotometer UV-160 I (Shimadzu) at OD_{595}.

3.4.2 Immunoprecipitation of hENDOV protein in cell lysates

Protocol:

Lysate preparation: 50 µl A/G-coupled agarose beads (Santa Cruz Biotechnology, sc-2001) per immunoprecipitation was blocked with 5% BSA (w/v) in RIPA lysis buffer for 1 hour rotating at 4°C. The beads were then washed 2x5 minutes in RIPA lysis buffer. The beads were resuspended to 50 % slurry in RIPA lysis buffer without PMSF and protease inhibitor cocktail. 2 mg of HeLa-S3 and HaCaT cell lysates were diluted in 1 ml RIPA lysis buffer and added with 1 µg of anti-hENDOV (Abcam, anti-FLJ35220). 60 µg of the four EGFP cell lysates from HeLa-S3 were also diluted in 1 ml RIPA lysis buffer and added 1 µg anti-hENDOV from Abcam. The mixtures were let to rotate for 1 hour.

Immunoprecipitation (IP): 50 µl of the 50 % slurry A/G-coupled agarose beads were added to each aliquot and rotated at 4°C for 1 hour. The mixtures were centrifuged briefly to collect beads and the lysate was discarded. The coated beads were washed in RIPA lysis buffer 3x5 minutes and once with 50 mM Tris pH 8.0 with rotation at 4ºC. 20 µl of 2x Sample buffer (10 µl NuPAGE® LDS Sample Buffer (4X) (Life Technologies), 4 µl 1 M DTT, and 6 µl MQ H2O) were added to pellets and boiled at 95º C for 5 minutes. The supernatants were carefully collected and load onto a NuPAGE® 12 % Bis-Tris gel (Life Technologies). Alternatively, the supernatant samples were collected, transferred to clean tube and frozen at -80º C for later use. The frozen supernatants were reboiled for 5 minutes prior to loading on a gel.

3.4.3 Protein analysis by SDS-PAGE and Western blotting

Western blot is a method developed to detect specific proteins in a lysate by using a primary antibody specific for the protein of interest and using a standard secondary antibody to detect the primary antibody for visualization on the membrane. The presence of sodium dodecyl sulphate (SDS) denatures the proteins and supplies a negative charge that is proportional to the number of amino acids and therefore allows for spreading of proteins by size during electrophoresis (Shapiro and Shiuey 1969).

SDS-PAGE gel electrophoresis protocol: Samples of recombinant hENDOV FL protein (25 ng and 50 ng) and cell lysates from HeLa-S3 and HaCaT (2 mg) that had not been immunoprecipitation were mixed with 2.5 µl NuPAGE LDS Sample Buffer (4X), 1.0 µl 1 M DDT and MQ H_2O to a total volume of ~10 µl. All the solutions were denatured at 95°C for 5 minutes, before they were applied to a 12% NuPAGE gel with NuPAGE MOPS (1X) buffer. 5 µl SeeBlue Plus2 Pre-Stained Standard (Life Technologies) was used as a marker. 20 µl of the samples that had been immunoprecipitation were loaded slowly to the bottom of the wells. Electrophoresis was performed: 150V for 40-60 minutes.

Protein blotting-Western blotting procedure: After gel electrophoresis were the proteins blotted using the iBlot® Gel Transfer Device (Life Technologies) onto PVDF membranes. The blotting was carried out as described in the manufacturer's instructions.

Antibody incubation procedure:

1. The membrane was removed from the transfer unit and blocked with PBS-T containing 5 % (w/v) skim milk (Blocking buffer) for 1 hour at room temperature with shaking.
2. Incubated the membrane with primary antibody against anti-hENDOV or anti-GFP diluted 1:1000 in blocking buffer.
3. The membrane was washed 3x10 minutes with 15 ml PBS-T.
4. The membrane was incubated for 1 hour at room temperature on shaker with the secondary antibody conjugated to HRP in blocking buffer.
    a. The membranes incubated with anti-hENDOV made by immunization of rabbit were incubated with rabbit anti-Goat IgG H&L (Biotin) secondary antibody (Abcam, ab6740) 1:30 000 dilution.
    b. The membranes incubate with anti-mouse antibody were incubated with goat anti-mouse antibody conjugated to HRP (Jackson ImmunoResearch, 115-036-068) in a 1:20 000 dilution.
5. Step 3 was repeated.
6. The membrane was added with 1 ml/membrane of Immun-Star WesternC chemiluminescence developing solution (BioRad).
7. ChemiDoc MP System (BioRad) was used to develop the membrane.

3.5 Confocal microscopy for intracellular localization of hENDOV protein

Confocal laser scanning microscopy is a method to visualize intracellular localization of proteins in intact cells. Because of the point scan/pinhole detection system, light contribution from the neighbourhood of the scanning spot in the specimen can be eliminated, allowing high Z-axis resolution. Fluorescence detection by sensitive photomultiplier tubes allows usage of filters with narrow bandpath, resulting in minimal overlap between two spectra. This is particularly important when demonstrating intracellular localization of protein with multicolour labelling.

3.5.1 Immunocytochemistry (ICC)

Immunocytochemistry (ICC) is a technique used to assess the presence of a specific protein or antigen in cells (cultured cells, cell suspensions) by use of a specific antibody binding to the target, thereby allowing visualization and examination under a microscope.

Procedure:

Preparation of cell culture in chamber slides:

The HeLa-S3 cell line was seeded 2.3 x 10^4 cells/well in a final volume of 200 µl medium in Lab-Tek 8-well chamber slides (Nunc, 177402), and let for overnight incubation to ensure good attachment to the slides.

Transient transfection of HeLa-S3 cell line:

The cells were then transient transfected with the three pEGFP-hENDOV constructs and pEGFP-N1 as described in Section 3.3.4 in a 3:1 ratio to DNA (1 µg DNA with 3 µl FuGENE6 for the chamber slides).

Cytotoxic effects of drugs on transient transfected cells:
24 hours post-transfection the transient transfected cells were exposed to DNA damaging agents. The various DNA damage agents and concentrations are listed in Table 3.2. The cells were then acutely exposed for the various agents for one hour.

1. The medium was removed and the drugs of interest were added to the cells diluted in 200 µl medium.
2. A control well containing the same volume of the dissolvent only (dimethyl sulfoxide (DMSO)) was added to the cells diluted in 200 µl medium.
3. The cells were then incubated 1 hour.

Table 3.2 DNA damage agents used.

Drugs/agents	Concentration
Camptothecin (CPT)	1.0 and 2.0 µM
Methyl methanesulfonate (MMS)	0.5 and 2.0 µM
Mitomycin C (MMC)	0.5 and 0.75 µg/ml
Bleomycin	5.0 and 10 µg/ml
Gamma rations	3 and 8 Gy

Fixation:

1. The medium was removed and the cells were rinsed once with PBS.
2. Cells were then fixed with 4% paraformaldehyde in PBS for 15 min at room temperature, then washed twice with ice cold PBS.

Pre-treatment and permeabilization:

3. The samples were quenched in 20 mM glycine in PBS for 10 min at RT.
4. Cells were then permeabilized with 0.1% Triton X-100 in PBS for 10 min at RT.
5. The cells were then washed three times in PBS for 5 min at RT.

Blocking and incubation:

6. Cells were blocked with 10% FBS in PBS for 30 min at RT.
7. The cells were incubated with mouse monoclonal anti-Fibrillarin (nucleoli marker) (Abcam, ab4566) diluted 1:100 in the 10 % FBS in PBS-T for 1 hour at RT or overnight at 4° C.
8. The solution was decanted and the cells were washed three times in PBS, 5 minutes each wash.
9. Incubated the cells with the secondary antibody Alexa Fluor 594 goat anti-mouse IgG (Life Technologies, A11005) diluted 1:1000 in 10 % FBS in PBS for 1 hour at RT in the dark.
10. The secondary antibody solution was decanted and the slides washed three times with PBS for 5 min in the dark.

Counter staining:

11. The samples were then incubated in 1:5000 dilutions with DAPI in PBS for 3 min.
12. Cells were then rinsed with PBS

Mounting:

13. The cells were mounted with a drop Mowiol medium (MERCK) to seal the coverslip to prevent drying and movement.
14. Slides were stored in the dark at 4°C.

3.5.2 Confocal laser scanning microscopy (CLSM)

Carl Zeiss LSM 510 CLSM was used for visualization of hENDOV protein.

1. The system was run with **Zeiss AIM 4.2**.
2. The combination of laser, barrier filters, and excitation dichroic mirrors were chosen to the following combination for FITC/Texas Red: laser combination: Ar488 nm + HeNe543 nm; barrier filters: BP 505-575 IR for channel 2, LP 560 for channel 3; dichroic mirror: HFT 488/543.
3. Objective used were **EC Plan-Neofluar 40x/1.30 Oil DIC M27.**
4. LMS-file format was used for image analysis and processing on **Zeiss LSM Image Browser**. The images of the cells were showed as a single view where the images were composed of the two channels.

3.6 Cell viability as measured by the MTT-assay

The MTT-assay (3-[4, 5-dimethylthiazol-2-yl]-2, 5-diphenyl tetrazolium bromide) is a sensitive colorimetric assay for the measurement of cell viability and cytotoxicity. The assay is based on the cleavage of the yellow tetrazolium salt, MTT, to form a soluble blue formazan product by a mitochondrial enzyme, and the amount of formazan produced is directly proportional to the number of living cells, present during MTT exposure. Since MTT assay is a rapid convenient, and economical, it has become a very popular technique for quantification of viable cells in culture. This assay is also broadly used to measure the *in vitro* cytotoxic effects of drugs on cell lines (Plumb 2004;Sylvester 2011). In this study early transformed and primary mouse embryonic fibroblast (MEF) *mEndoV* +/+ and *mEndoV* -/-, from now on referred to as MEF WT and MEF KO, respectively.

3.6.1 MTT-assay

Procedure:

1. **DAY ONE:** Both early transformed and primary MEF WT and KO cells were seeded into 96-well plates at concentrations of 3000-4000 cells/well in a volume of 100 µl medium. Both cell lines were left for incubation overnight to ensure good attachment to the plates.
2. The cells were plated in triplicates in each plate. Additional six wells containing only the medium were plated for measuring the background on the medium.
3. **DAY TWO:** 5 µl of drug (Table 3.3) was added to each well, and cells were incubated 48 hours. Three additional control wells containing the same volume of the dissolvent only was added to the cells.

Table 3.3 DNA damage agents used on cell viability in MEF cells.

Drugs/agents	Concentration (µM)	Dissolvent
Camptothecin (CPT)	0, 0.05, 0.1, 0.5, 1.0, 2.0, 4.0, and 6.0	Dimethyl sulfoxide (DMSO)
Methyl methanesulfonate (MMS)	0, 50, 100, 120, 140, 180, and 200	Medium
Mitomycin C (MMC)	0, 0.1, 0.5, 1.0, 5.0, 10, and 20	H2O MQ
Gamma rations	0, 20, 40, and 60 Gy	-

4. **DAY FOUR:** 10 µl 5 mg/ml MTT in PBS was added to each well and the plates were incubated 4 hours.
5. The cells were solubilized with 100 µl of the Solubilization solution (10 % SDS in 0.01 M HCl) added into each well. The plates were let to incubation overnight.
6. **DAY FIVE:** The absorbance was read with Wallac 1420 VICTOR^2 spectrophotometer at 550 nm with a reference filter of 690 nm.

4 Results

4.1 Different transcript variants of *hENDOV*,

Multiple sequence alignments of human *ENDOV* with *EndoV* from several other organisms from *T. maritime* to *M. musculus* have shown that EndoV is a highly conserved protein. Within different mammals EndoV is even more conserved (see Appendix III for multiple sequence alignments), all containing 9 or 10 exons. Data from the EST database show a variety of single-nucleotide polymorphisms (SNPs) identified in human genomes. (J. K. Lærdahl, unpublished data).

The NCBI Reference Sequence (RefSeq) annotates three representative transcripts of the Homo sapiens locus FLJ35220, encoding human Endonuclease V, NM_173627.3, NM_001164637.1, and NM_001164638.1. A presentation of all human ENDOV isoforms analysed in this thesis are summarized in the Table 4.1. The full DNA and protein sequences are listed in the Appendix I. Many different isoforms of the protein are listed in the human EST database[1]. However, of the three annotated human transcripts only one contains exon 3, suggesting that *hENDOV* can to be spliced differently compared to *EndoV* from other animals.

Table 4.1 Presentation of human EndoV isoforms.

Transcript name	Isoform	mRNA (bp)	Protein (aa)	Mass (kDa)	Exons present
NM_173627.3	1	2,840	282	30.8	1-9 (short), 10
NM_001164637.1	2	2,705	237	25.6	1, 2-9 (short), 10
NM_001164638.1	3	1,288	264	28.5	1, 2-9 (full length)

[1] http://www.ncbi.nlm.nih.gov/UniGene/clust.cgi?ORG=Hs&CID=389678

4.2 5'RACE and 3'RACE experiments

5'RACE and 3'RACE experiments using Marathon-Ready™ cDNA from human brain (Clontech) was used to identify the different transcript variants of *hENDOV*.

For 5'RACE reaction a gene specific primer (GSP1) located in exon 6/7 was used together with an outer primer (AP1) located in the adaptor at the 5' ends of the transcripts. For the 3'RACE reaction a gene specific primer (GSP2) located in exon 4 was used together with the AP1 primer located in the adaptor at the 3' ends of the transcripts (Figure 4.1). The expected sizes of RACE products amplified with GPSs are shown in Table 4.2. 5'RACE and 3'RACE cDNA products amplified with GSPs and AP1 appeared as many bands (Figure 4.2).

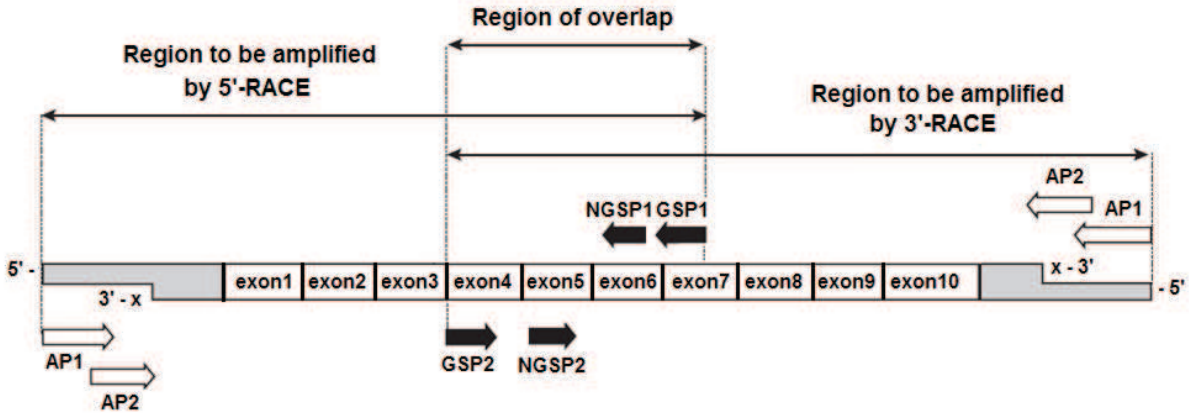

Figure 4.1. The cDNA template from human brain and primers used in Marathon RACE reaction. cDNA synthesis and adaptor ligation create a population of cDNA with the hENDOV structure depicted above. The exons that are represented show the different exons that are found in the different isoforms of hENDOV (this is a schemativ illustration where the width of the boxes aren't representative of the real size of the exons). Adaptor primes (AP1 and AP2). AP2 is for analysis of RACE products for nested RACE PCR. Gene specific primers (GSP1 and GSP2). Nested gene specific primer (NGSP1 and NGSP1) can be used for characterization of RACE products for nested RACE PCR.

Table 4.2 Size of RACE products amplified with GSPs.

GSP products	Primers	Description	Size (bp)
5'RACE	AP1/13254 (GSP1)	With exon 3	603
5'RACE	AP1/13254 (GSP1)	Without exon 3	468
3'RACE	13253 (GSP2)/AP1	With full length exon 9	509
3'RACE	13253 (GSP2)/AP1	With shot exon9 and exon 10	484

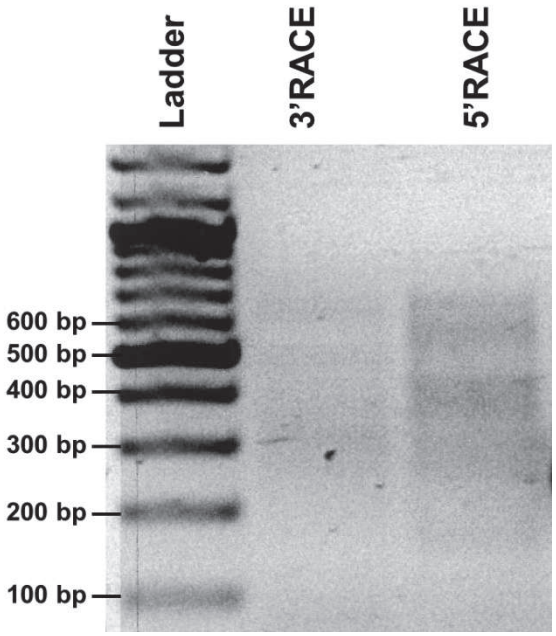

Figure 4.2. 3'RACE and 5'RACE cDNA product amplified with gene specific primers and adaptor primer visualized after gel electrophoresis.

Since a lot of weak bands were observed in the first RACE reaction we tried nested PCR in order to obtain more specific products. In nested PCR we used the first RACE reaction as a template for a second PCR using nested outer primer (AP2) and nested gene specific primers (NGSPs), downstream and upstream of the first primers as shown in Figure 4.1. The NGSP1 primer is located in exon 6 and the NGSP2 primer is located in exon 5. The expected sizes of RACE products amplified with NGPSs are shown in Table 4.3. A specific band was amplified for nested 3'RACE PCR product, but for nested 5'RACE PCR only low molecular weight products were present (Figure 4.3).

Table 4.3 Size of RACE products amplified with NGSPs.

NGSP products	Primers	Description	Size (bp)
5'RACE	AP2/13709 (NGSP1)	With exon 3	562
5'RACE	AP2/13709 (NGSP1)	Without exon 3	427
3'RACE	13708 (NGSP2)/AP2	With FL exon 9	562
3'RACE	13708 (NGSP2)/AP2	With shot exon9 and exon 10	431

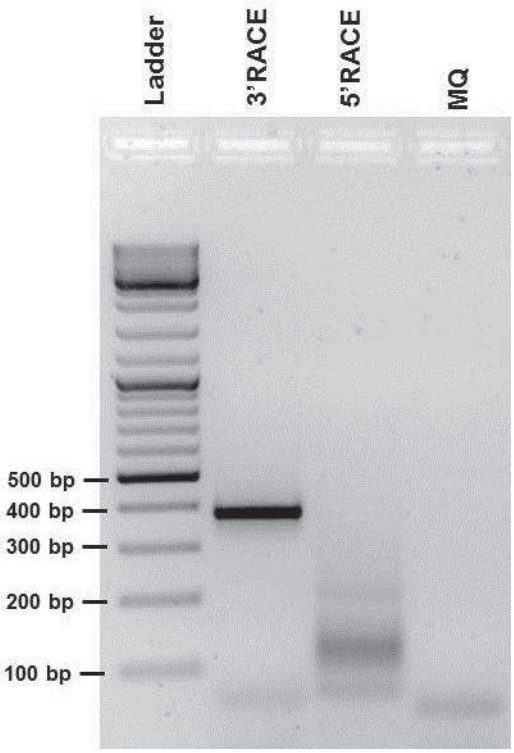

Figure 4.3. Nested 3`RACE and 5`RACE PCR products amplified with the nested gene specific primers and nested adaptor primers visualized after gel electrophoresis.

The nested 3'RACE PCR product slightly lower than 400 bp was obtained. The product was excised from the gel (Section 3.1.2)

Because no nested 5'RACE PCR product within the expected size was amplified, we decided to cut out two gel fragments from the first 5'RACE reaction, one fragment round 400 bp and the second fragment at round 600 bp, shown in the Figure 4.2.

The isolated RACE products were subcloned into the pCR®2.1-TOPO vector as described in methods. The enzyme *EcoRI* was used to digest of purified plasmid DNA for verification of insert size. All clones showed a variation in the sizes of the bands (data not shown). The samples of expected size were sequenced. DNA sequences were analysed and compared with the *hENDOV* gene in: NM_173627.3, NM_001164637.1, and NM_001164638.1 listed in Appendix I.

A total of 30 clones were sequenced in which only two clones contained exon 3, 10 clones were partially unprocessed containing introns, and 7 were degraded (starting in exon 4 or 5). 11 of 30 sequenced clones were lacking exon 3, were 2 and 1 of these clones were without exon 4 and exon 5, respectively. Based on these observations we assume that full-length clones of hENDOV containing exon 3 most likely are expressed at low levels in the cells.

The specific band we obtained from nested 3'RACE PCR and subcloned into pCR®2.1-TOPO vector showed that the adaptor on 3' end was found in the same place in exon 8 of the 5 sequenced clones. This will not tell us whether we can find protein of hENDOV with short or full length exon 9 or exon 10.

4.3 Expression analysis of the three transcript variants of *hENDOV*

In order to further clarify the expression of the different transcript variants of *hENDOV* in the cell, we used cDNA isolated from ACHN cell line (obtained from Dr. Yang Mingyi) for PCR analysis using exon-specific primers (Section 3.2). Amplifications with of all the exon-specific primers were successful (Figure 4.4) and shows that the exons in the three annotated *hENDOV* transcripts are present in the cells.

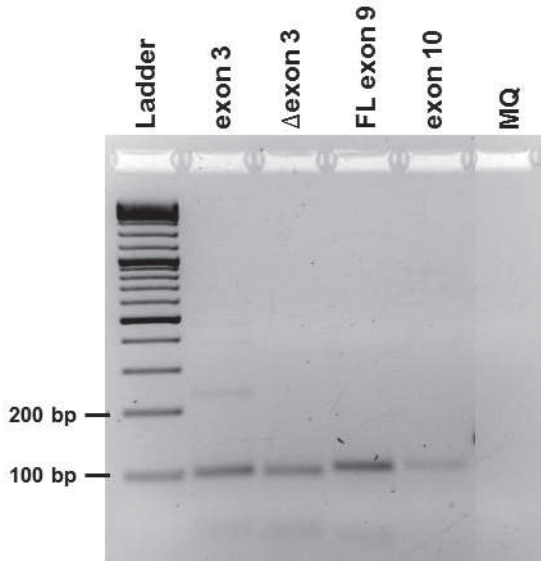

Figure 4.4. PCR amplification of the by exon-specific primers. The PCR amplifications were used with specific primers for exon 3 (13735/13737), without exon 3 (13738/13739), full length exon 9 (13740/13641), and for short exon9 + exon 10 (13742/13743).

4.4 Immunoprecipitation of endogenous hENDOV

Immunoprecipitaion was conducted to examine the endogenous protein with respect to size (+/- exon 3) and possible post-translational modifications. First a test was run on an antibody made by immunization of rabbits with our purified recombinant hENDOV FL (isoform 1). This was done by Western blot on purified hENDOV FL protein. Serum from two different rabbits (rabbit 132 and 133) were used: the small bleed (PP), large bleed (GP), and the serum for the final bleed (SAB). The results (Figure 4.5) show that serum from GP132 had best binding effect and was therefore used in the further experiments. The hENDOV FL has an estimated size of 34 kDa.

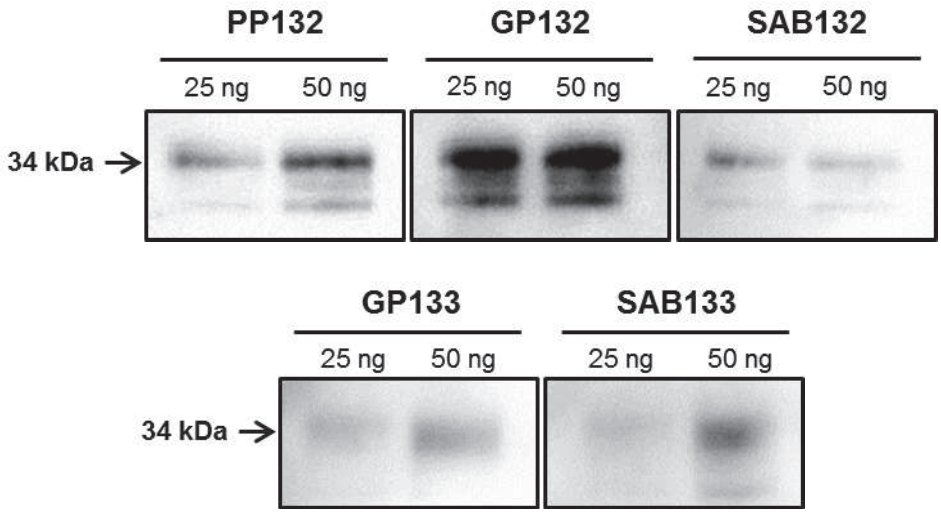

Figure 4.5. Test of the antibody made by immunization of rabbits on pruified hENDOV FL protein by Western analysis. The on purified hENDOV FL proteins is blotted onto PVDF membranes and probed with serum from two different rabbits (rabbit 132 and 133): the small bleed (PP), large bleed (GP), and the serum for the final bleed (SAB).

The immunoprecipitation was conducted with protein A/G PLUS-agarose beads as described in methods. Lysate from HeLa-S3 and HaCaT cells were immunopresipitated using beads conjugated with anti-hENDOV (Abcam, anti-FLJ35220, ab69400). The precipitated material was run on SDS-PAGE gel, and subjected to Western analysis using the hENDOV antibodies, one obtained from Abcam and the antibody made by immunization of rabbit (GP132).

No immunoprecipitated endogenous hENDOV protein was detected with either of the two types of antibodies in HeLa-S3 and HaCaT cell lysates, as shown in Figure 4.6 A and B.

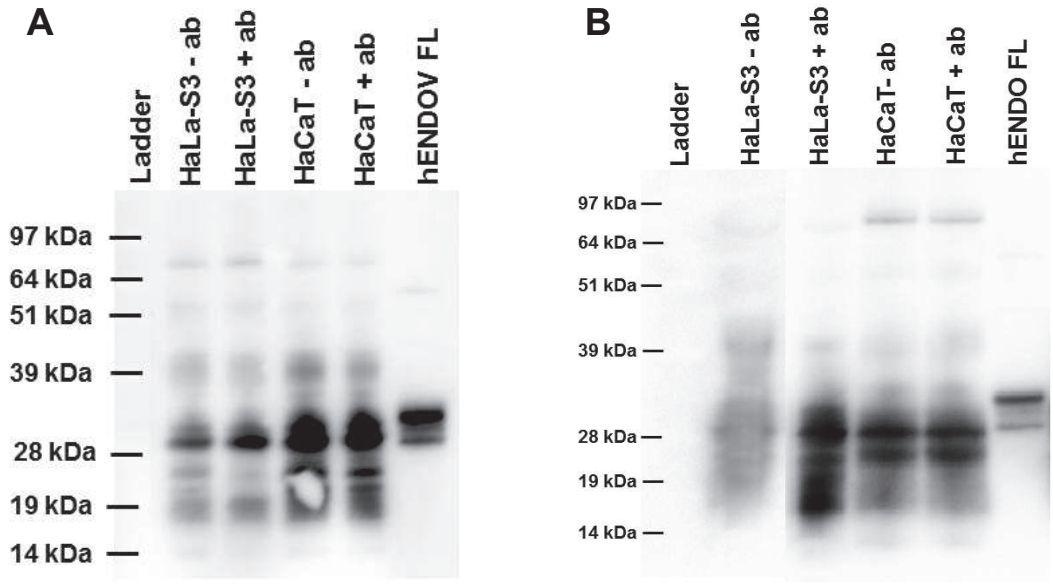

Figure 4.6. Western analysis of immunoprescipitated endogenous hENDOV protein. Lysate from HeLa-S3 and HaCaT cells were immunopresipitated with beads conjugated with antibody against hENDOV (anti-FLJ35220). (A) The PVDF membrane was probed with anti-hENDOV obtained from Abcam, anti-FLJ35220. (B) This membrane is probed with the serum from rabbit, GP132.

4.5 Intracellular localization of EGFP-hENDOV fusion protein

Enhanced GFP (EGFP) is a commonly used tag to label proteins for localization studies in plants (Grebenok et al. 1997;Von Arnim et al. 1998), yeast (Bordonne 2000), and mammals (Borghi et al. 2001;Minopoli et al. 2001;Sheng et al. 2004), e.g. to identify nuclear localization.

Syntetic cDNA for *Homo sapiens* Endonuclease V transcript variant 1-3 was subcloned by Genscript in a pEGFP-C1 vector. These vectors were used to express EGFP-hENDOV fusion protein in HeLa-S3 cells. Transfections were carried out using FuGENE 6. Before analysis, cells were cultured for twenty-four hours post-transfection. The cells were then fixed with 4 % paraformaldehyde and observed under a confocal microscope.

This was done to monitor of how the different hENDOV isoforms of the proteins would localize inside the cells. All three of the pEGFP plasmids constructs and vector only (pEGFP-N1) were transfected into HeLa-S3 cell line. The result of cellular localization is shown in the Figure 4.7 below.

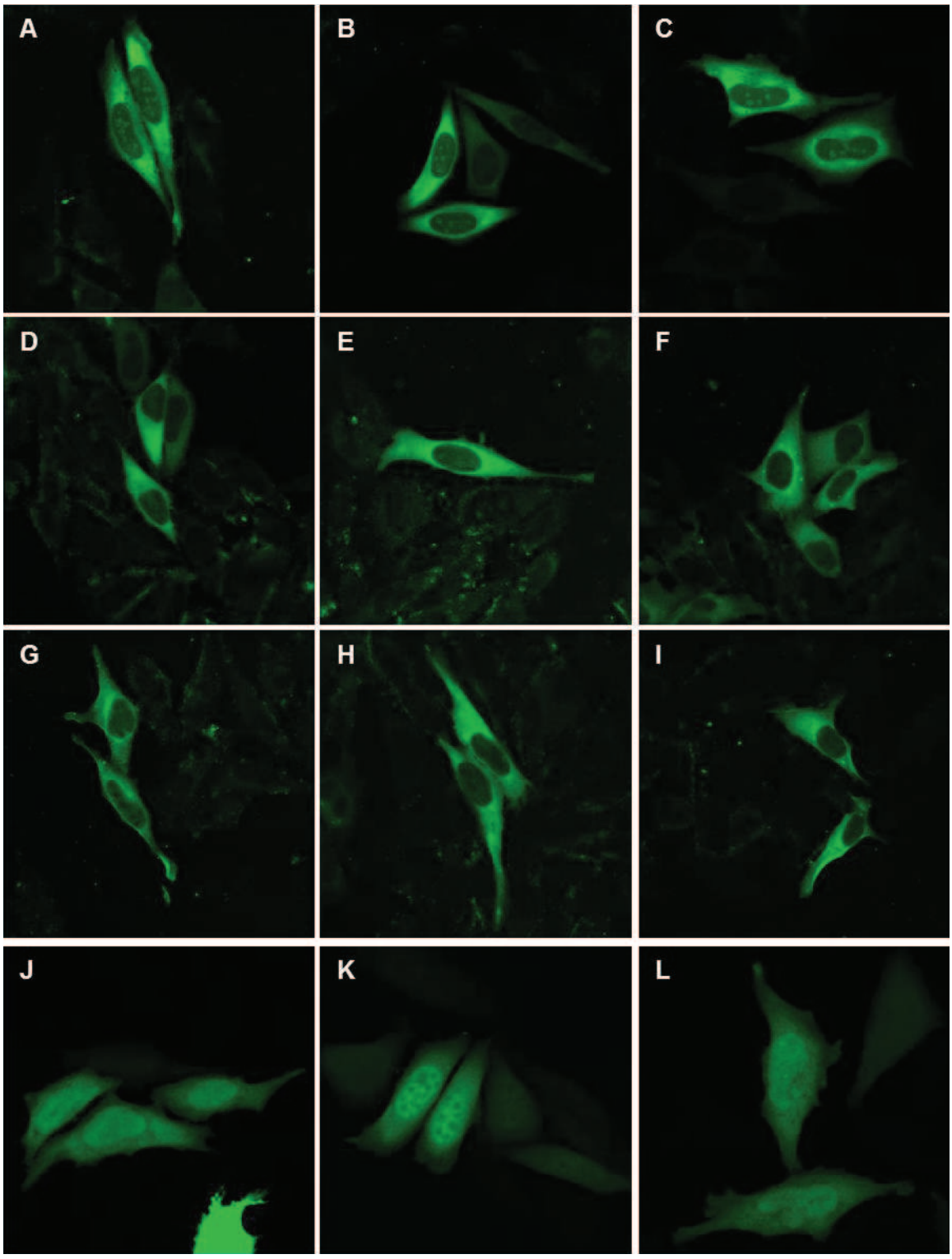

Figure 4.7. Subcellular localization of EGFP-hENDOV isoform 1-3. A triplicate representative panels of HeLa-S3 cells following transient transfection, as viewed by laser scanning confocal microscopy. (A-C) Shows cells expressing EGFP-hENDOV isoform 1 localized in the nucleus and in the cytoplasm, (D-F) EGFP-hENDOV isoform 2, shows only localization of the fusion protein in cytoplasm, (G-I) EGFP-hENDOV isoform 3 showed also only localization of the fusion protein in cytoplasm, and (J-L)EGFP only shows localized in the nucleus and cytoplasm of transfected cells.

EGFP-hENDOV isoform 1: This protein has exon 3 and a short exon 9, and exon 10 (Figure 4.7 A-C). This construct showed localization in the nucleus and in the cytoplasm. The localization in the cell nucleus was at distinct compartments corresponding to nucleoli. To verify this localization the cells were stained with a specific antibody against fibrillarin, a protein found only in this compartment. Figure 4.8 shows that EGFP-hENDOV isoform 1 protein is enriched in nucleoli as it co-localizes with fibrillarin antibody.

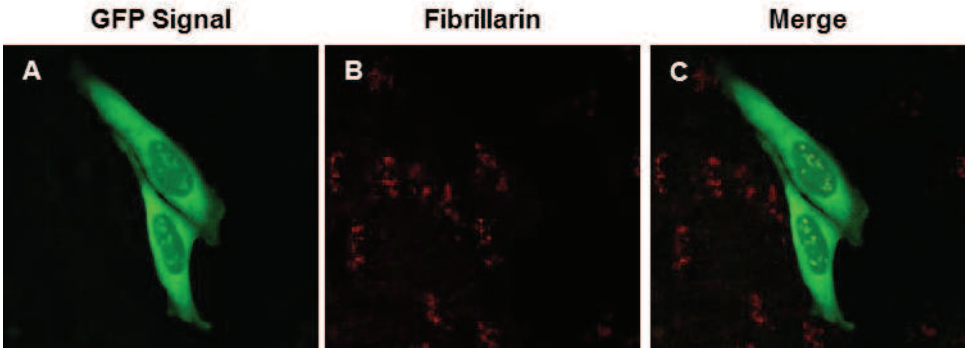

Figure 4.8. Subcellular localization of EGFP-hENDOV isoform 1 and fibrillarin. (A) Shows the localization of EGFP-hENDOV in the nucleus and in the cytoplasm. (B) The cells are stained with a specific antibody against fibrillarin. (C) Shows a merged picture of EGFP-hENDOV isoform 1 protein enriched in nucleoli as it co-localizes with fibrillarin antibody.

EGFP-hENDOV isoform 2: This protein is without exon 3, has a short exon 9, and exon 10 (Figure 4.7 D-F). This isoform of hENDOV showed only localization of the fusion protein in cytoplasm.

EGFP-hENDOV isoform 3: This protein is also without exon 3 and has the full length form of exon 9 (Figure 4.7 G-I). This showed also only localization of the fusion protein in cytoplasm.

EGFP only (pEGFP-N1) (Figure 4.7 J-L) was localized in the nucleus and cytoplasm of transfected cells.

No difference in localization pattern was seen when the GFP-tag was placed at the C-terminal end of the protein. These data demonstrate that full-length hENDOV with exon 3 may exert its function in nucleolus and possibly also in cytoplasm. The putative truncated form of hENDOV lacking exon 3, however, is most likely not associated with DNA handling/processing.

4.6 Western analyse GFP fusion proteins

Western analysis was performed to confirm that the various EGFP fusion proteins were expressed in their full length in the cells.

The protein analysis by SDS-PAGE and Western blotting of the transient transfected HeLa-S3 cells overexpressing the three different EGFP fusion proteins are shown in Figure 4.9. The three different proteins, EGFP-hENDOV isoforms 1-3 were visualized by probing the blots with anti-GFP antibody. Bands of expected sizes for all proteins were detected: EGFP only (pEGFP-N1) (positive control, 27 kDa), EGFP-hENDOV isoform 1 (57.8 kDa), EGFP-hENDOV isoform 2 (52.6 kDa), and for EGFP-hENDOV isoform 3 (55.5 kDa).

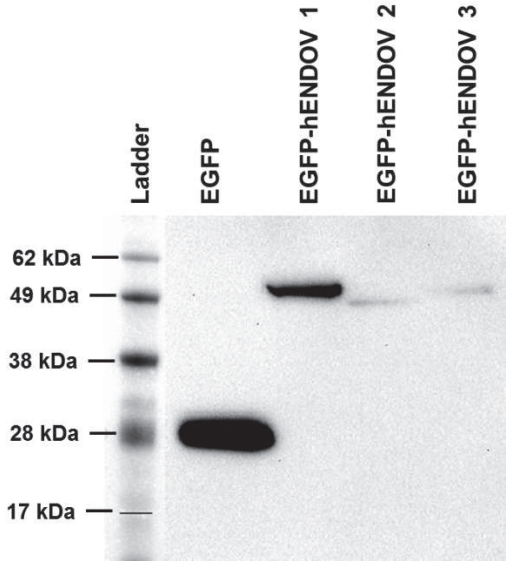

Figure 4.9. Detection of the three different isoforms of EGFP-hENDOV HeLa-S3 cells lysates. SDS-PAGE gel and Western blotting of cell lysates overexpressed with the three EGFP-hENDOV proteins blotted onto PVDF membranes and probed with anti-GFP antibody.

4.7 Relocalisation of EGFP-hENDOV isoform 1

The nucleolus (plural nucleoli) is the most active and dynamic nuclear domain that plays a prominent role in the organization of various components of the nucleus. The major roles of nucleus: ribosome biogenesis, rDNA transcription, pre-rRNA processing, and assembly for mature rRNAs with ribosomal proteins (Hadjiolov 1985). Nucleoli are essential in the formation of ribosomes that synthesize cell proteins.

Based on the specific nucleoli localization of the EGFP-hENDOV isofrom 1 fusion protein, relocalisations of hENDOV after treatment of cells with DNA damaging agents were studied. Initially, camptothecin (CPT) which is a DNA topoisomerase I inhibitor, was chosen. CPT is thought to induce DSBs in a DNA replication dependent manner.

Before analysis, cells were cultured for twenty-four hours post-transfection; the cells were treated with 1 μM and 2 μM CPT for 1 hour before examination under a microscope. We observed that the nucleoli localization was excluded from the nucleus after 1 hour with acute treatment of 1μM and 2 μM CPT (Figure 4.10, C and D).

Next, the cells were treated with gamma radiation which induced clean DSBs in the DNA. Cells were radiated with 3 Gy and 8 Gy before fixation with 4 % paraformaldehyde. These acute treatments did not result in relocalisation of hENDOV in HeLa-S3 cells (Figure 4.10, E and F).

Then we looked at cells treated with bleomycin which results in DSBs. The cells were incubated with 5μg/ml and 10μg/ml bleomycin (Figure 4.10, G and H) for 1 hour prior to fixation with 4 % paraformaldehyde. The next drug that was tested was Mitomycin C that causes alkylation damage and DNA DSBs. Cells were incubated with 0.5 μg/ml and 0.75 μg/ml Mitomycin C (Figure 4.10, I and J). The last drug tested for relocalization of hENDOV isoform 1, was methyl methanesulfonate (MMS), 0.5 mM and 2.0 mM. (Figure 4.10, K and L) MMS can also cause alkylation damage and DSBs. Neither of the treatments results in relocalisation of EGFP-hENDOV isofrom 1 in transient transfected HeLa-S3 cells.

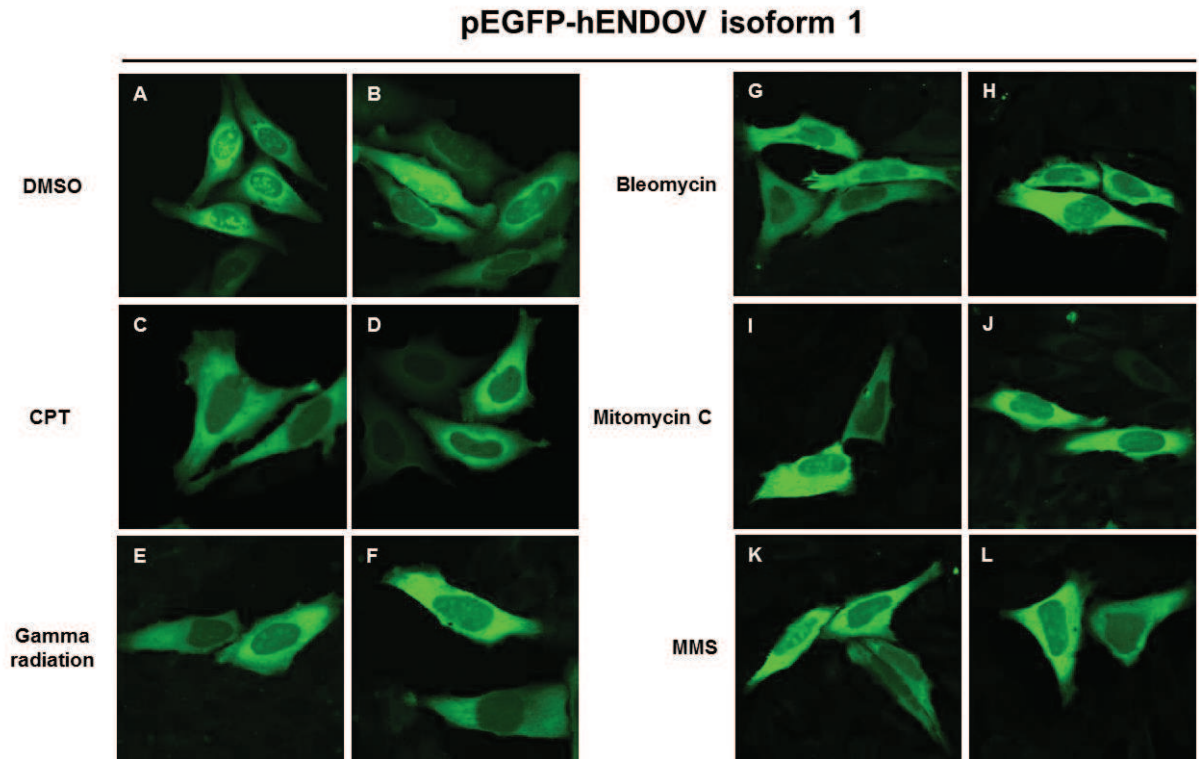

Figure 4.10. EGFP-hENDOV isoform 1 expressed in HeLa-S3 cells treated with different DNA damageing agents. (A-B) Transfected cells with DMSO (control). (C-D) Transfected cells treated with CPT, 1 µM and 2 µM, respectively. (E-F) Cells exposed with 3 and 8 Gy gamma radiation, (G-H) 5 and 10 µg/ml Bleomycin, (I-J) 0.5 and 0.75 µg/ml Mitomycin C, and (K-L) 0.5 and 2.0 µM MMS.

Based on the relocalization of nucleoli localization after acute treatment with CPT, we wanted to see if the nucleoli were intact. To verify this, cells were stained with antibody against fibrillarin. Confocal microscopy pictures showed that the nucleoli remained intact after the CPT treatment (Figure 4.11).

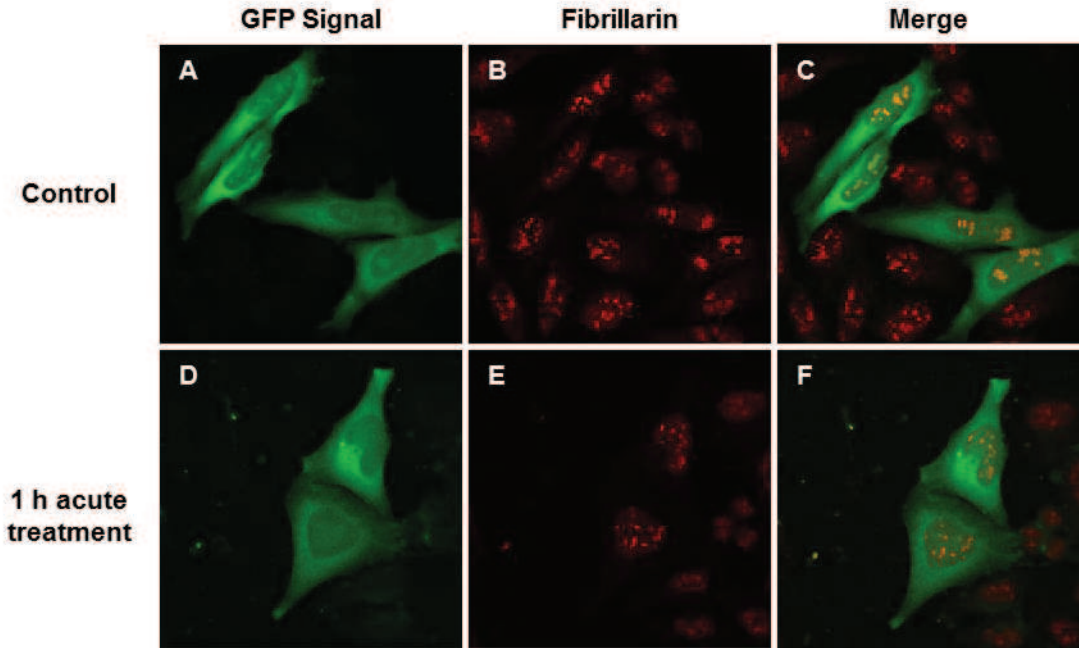

Figure 4.11. EGFP-hENDOV isoform 1 over expressed in HeLa-S3 treated with 2µM CPT. (A-C) The cells are in incubated with DMSO, this is the solvent of CPT. (D-F) 1 hour with acute treatment of 2 µm CPT.

4.8 Viability assay (MTT-assay)

In our laboratory we have generated constitutive knockout mice of *mEndoV* from which we have isolated the primary mouse embryonic fibroblast (MEF) cells. Studies of MEF cells have played an important role in the elucidation of the molecule mechanisms underlying cellular immortalization, transformation, and tumorgenesis. Additionally, utilization of MEF cells disrupted for specific gene has provided a powerful tool to analyse the genetic regulation of these cellular processes (Sun and Taneja 2007).

Viability assay was used in cytotoxicity studies to see whether we can observe a difference between the MEF cell lines in which the gene for mouse *EndoV* were intact and knocked out. MTT-assay technique has become a popular quantification of viable cells in culture. For each cell line optimal seeding concentration were tested, to obtain maximal possible absorbance while ensuring that cells remained in exponential growth. The cell number chosen for early transformed MEF (passage around 18-25) and primary MEF (passage 1-5) cells was 3000-4000 cells/well for 5-days assay.

4.8.1 Early transformed MEF

Based on the relocalization of nucleoli localization after acute treatment with CPT of EGFP-hENDOV isoform 1 where nucleoli were excluded from the nucleus in transient transfected HeLa-S3 cells. We analysed the effect of CPT on viability of without MEF KO compared to MEF WT cells. This was done on early transformed MEF cells. Raw data for all the graphs in this study is listed in Appendix II. As shown in Figure 4.12, a wide variation was observed within the four different lines that were tested by WT and KO cell line showing that the transformed cell lines behaves differently.

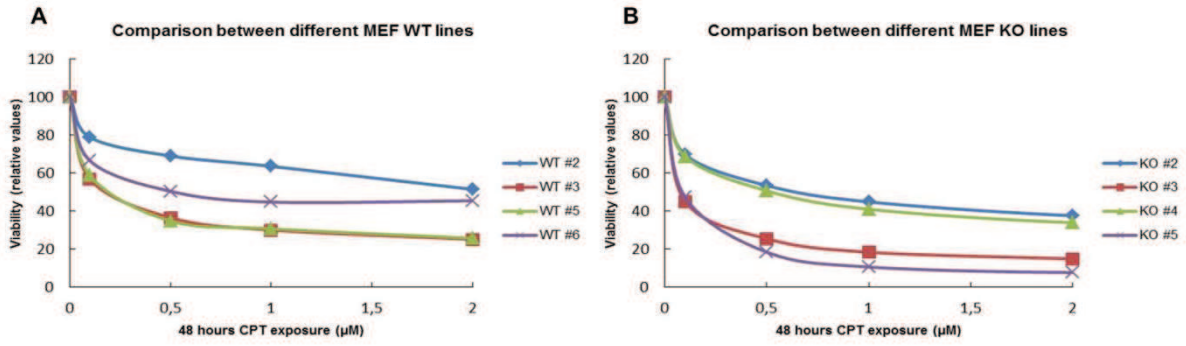

Figure 4.12. Dose response curved for the early transformed MEF WT and KO cell lines exposed to different doses of CPT (µM) after 48 hour incubation. (A) Shows the variation in dose response between the four early transformed MEF WT cell lines used in this study. (B) Shows the variation in dose response between the four early transformed MEF KO cell lines.

An average of the viability data for the MEF WT and the KO on the early transformed cell lines was estimated. However no difference was seen between the cell lines with *mEndoV* gene intact and with the same cell lines with *mEndoV* gene knocked out (Figure 4.13).

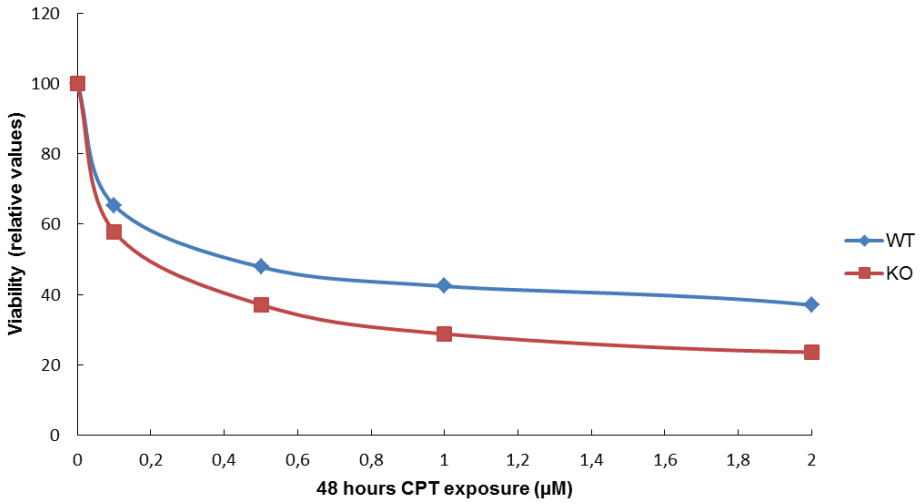

Figure 4.13. The estimated average of dose response curved for comparison of the early transformed MEF WT and KO cell lines exposed to different does of CPT (µM) after 48 hour incubation.

4.8.2 Primary MEF

Because there was considerable variation within each early transformed MEF cell line, a study was also done on the corresponding primary MEF cell lines. The variation observed within each primary MEF cell lines is much lower compared to the early transformed MEF lines. This was also observed in all the five different lines that were tested by each WT and KO cell line (Figure 4.14).

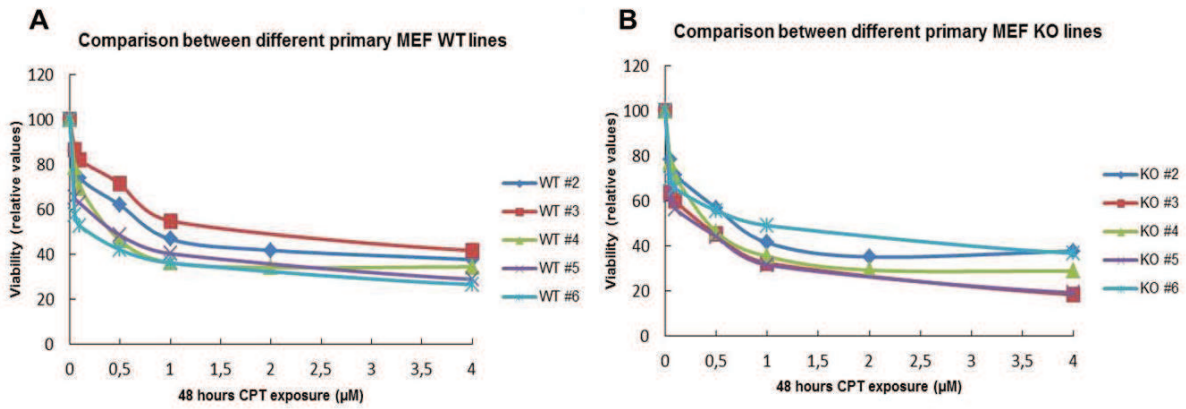

Figure 4.14. Dose response curved for the primary MEF WT and KO cell lines exposed to different doses of CPT (µM) after 48 hour incubation. (A) Shows the variation in dose response between the five primary MEF WT cell lines used in this study. (B) Shows the variation in dose response between the five primary MEF KO cell lines.

However, when the average of the viability data for the MEF WT and KO primary cell lines was calculated, no difference was seen between cell lines with or without *mEndoV* (Figure 4.15).

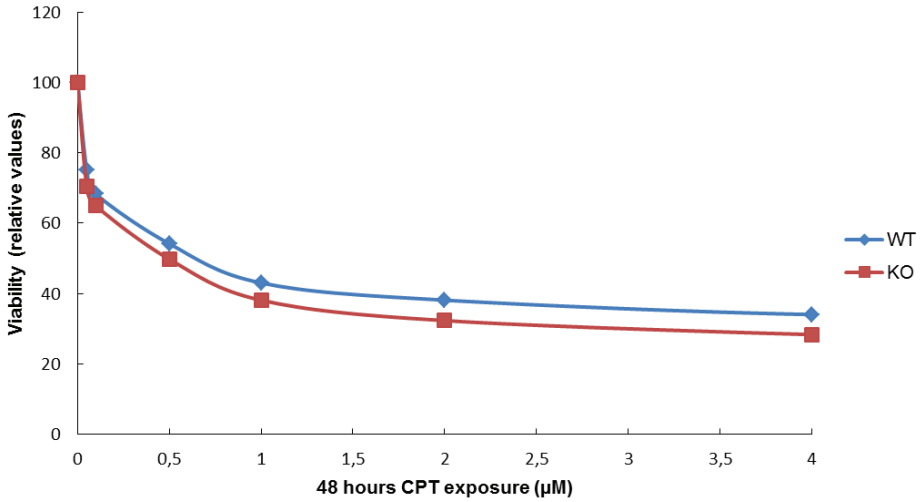

Figure 4.15. The estimated average of dose response curved for comparison of the primary MEF WT and KO cell lines exposed to different does of CPT (µM) after 48 hour incubation.

4.8.3 Viability assay (MTT-assay) with different DNA damaging agents

Since no effect was observed by exposing MEF Endo V cell lines to CPT treatment, assays with other agents were also performed. Cells were incubated with methyl methanesulfonate (MMS), Mitomycin C (MMC), and gamma radiation as described in Methods. As one can see from Figure 4.16-18 no difference in viability was observed between the primary MEF Endo V WT and KO cells when exposed to these agents.

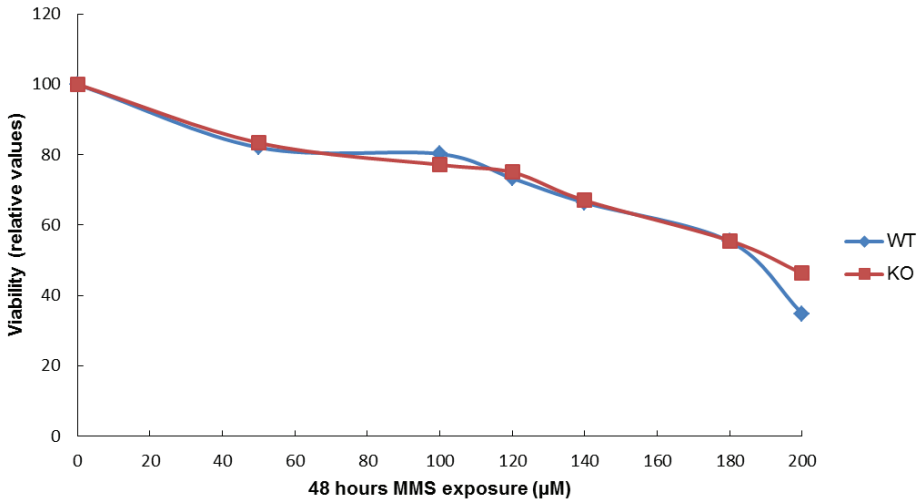

Figure 4.16. The estimated average of dose response curved for comparison of the primary MEF WT and KO cell lines exposed to different doses of MMS (µM) after 48 hour incubation.

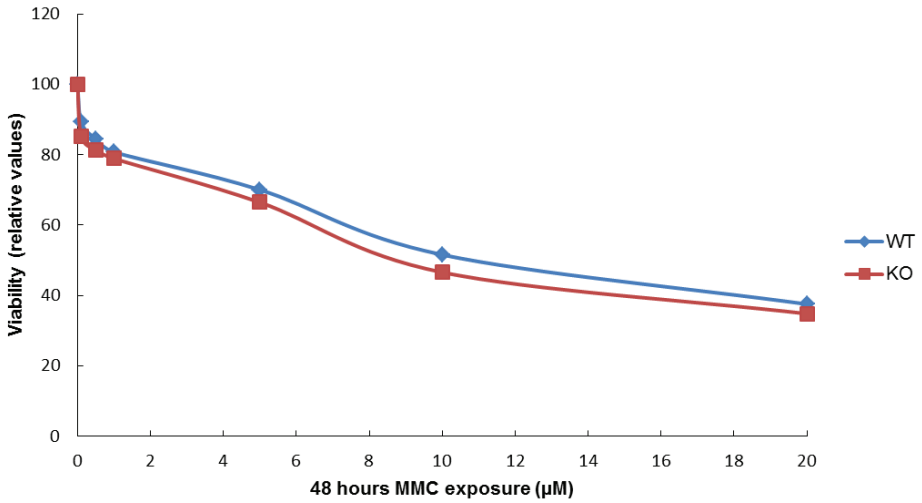

Figure 4.17. The estimated average of dose response curved for comparison of the primary MEF WT and KO cell lines exposed to different doses of MMC (µM) after 48 hour incubation.

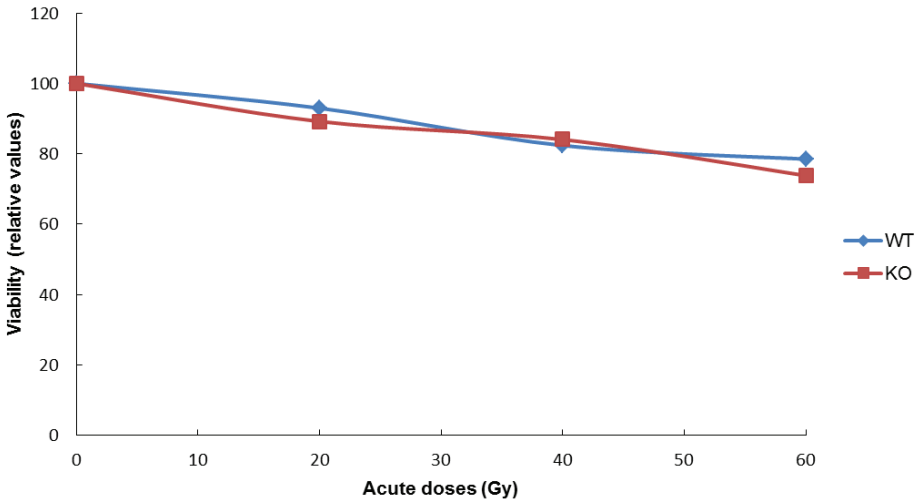

Figure 4.18. The estimated average of dose response curved for comparison of the primary MEF WT and KO cell lines exposed acute doses exposure gamma ratiation (Gy) after 48 hours recovery**.**

5 Discussion

5.1 Different transcript variant of *hENDOV*

The reason for the 5'RACE and 3'RACE experiments being conducted were based on observations done by others in the lab where they looked at the total RNA that was purified from primary human fibroblasts, kidney (ACHN), and colon (HCT116) cell lines and subjected to cDNA synthesis and PCR analysis using exon 1 and exon 8 or exon 9-specific primers. They were only able to amplify *hENDOV* transcripts lacking exon 3. This was further demonstrated in 5'RACE experiments using Marathon-Ready™ cDNA from brain in which only 2 of 30 sequenced clones contained exon 3. Based on these observations we assume that full-length *hENDOV* transcript containing exon 3 most likely are expressed at low levels in the cells. The 3'RACE experiments gave no clarification of the hENDOV expression since the inserted adaptor (done by Clontech) was found in exon 8, within the area that we wanted to look at.

Of the 30 sequenced clones from the 5'RACE analysis: 10 clones were partially unprocessed containing introns, and 7 were degraded (starting in exon 4 or 5). A few percent of the population has a stop codon in exon 3. This would cause an extremely short version of hENDOV which would most likely be non-functional. 25 % of an Asian panel has a *hENDOV* variant with an A to G mutation just in front of exon 4. This removes the 3'splicing signal for intron 3, and most likely deleterious for the whole protein (J. K. Lærdahl, unpublished data). Many different isoforms of the protein are listed in the human EST database. This includes at least 31 spliced variants, indicating a highly complex locus. However, of the three annotated human transcripts only one contains exon 3, suggesting that *hENDOV* appears to be spliced differently compared to *EndoV* from other animals.

The expression of *hENDOV* transcript variant 2 (lacking exon 3) in human fibroblast cDNA library is confirmed by others in the laboratory. But the functions of the corresponding proteins are obscure since they lack exon 3, which is known to make up the core of the protein. The missing exon also contains the conserved PYVS motif. This motif is believed to act as a DNA strand-separating wedge, and is thus important for DNA binding. It would be of interest to test this isoform for DNA binding capability in the same way as the hENDOV isoform 1. Unfortunately, soluble free hENDOV isoform 2 has not been obtained, however optimisation to the purification protocol is on-going.

We were able to amplify the three annotated *hENDOV* transcripts with a PCR amplification with cDNA isolated from ACHN cells using exon 3, without exon 3, full length exon 9, and shot exon 9 + 10 specific primers. This shows that the transcripts are present, but says nothing about the quantitative amount in the cell. Due to the time aspect of this thesis, we did not have time to do the Real-Time qPCR to quantify the amount of the three different transcripts to the total level of *hENDOV* transcripts in normal cells.

5.2 Western analysis of endogenous hENDOV

We could not detect endogenous hENDOV protein in the Hela-S3 and HaCaT cell lysates by immunoprecipitation. This might be that the level of hENDOV in these cells is too low to be detected with the specific antibodies.

There are several factors that can lead to the negative result that was obtained using immunoprecipitation. The ionic strength (salt concentration) or choice of detergent and pH in the lysis buffer may significantly affect the protein interactions and/or the structural integrity of the protein. Additionally, steric hindrance from the epitope area on the antibody may interfere with the protein interactions. Another consideration is that immunoprecipitation contains several wash steps and incubation periods where the protein interaction might be disrupted or the proteins degraded by proteases. These problems can be reduced by adding protease inhibitors to the lysis buffer and preforming the incubations at 4°C.

Non-specific binding to the beads is a common problem. Addition of detergents such as Tween and Triton X-100 to the washing buffer can reduce the amount of protein that bind in a non-specific manner. In addition, the incubation time can be reduced and the primary antibody concentration can be decreased. Blocking with skimmed milk or BSA could also reduce the number of binding sites in the beads.

5.3 Intracellular localisation

The cells of eukaryotic organisms are elaborately subdivided into functionally distinct membrane bound compartments. Some major constituents of eukaryotic cells are: extracellular space, cytoplasm, nucleus, mitochondria, Golgi apparatus, endoplasmic reticulum (ER), peroxisome, vacuoles, cytoskeleton, nucleoplasm, nucleolus, nuclear matrix and ribosomes.

The green fluorescent protein (GFP) from the jellyfish *Aequorea victoria* has vaulted from obscurity to become one of the most widely studied and exploited proteins in biochemistry and cell biology. The protein's ability to generate a highly visible, efficiently internal fluorophore is very valuable. GFP has become well established as a marker of gene expression and protein targeting in intact cells and organisms (Tsien 1998). Nevertheless, EGFP alone is distributed in the cytoplasm and nucleus, and this can give a diffuse conclusion about NLS in the fusion partner (Bohm et al. 2006).

Intracellular localisation of a protein can provide valuable information towards elucidating the biological function. In this study the subcellular localization of the three isoforms of hENDOV fused to EGFP was investigated. However, the intranuclear localisation differs between the three proteins. We showed that hENDOV isoform 1 was located to the cytoplasm and nucleus with enrichment in nucleoli, whereas the other two proteins showed only localization in the cytoplasm. Cells overexpressing EGFP-hENDOV isoform 1 were exposed to DNA damaging agents and interestingly after CPT exposure hENDOV was excluded from the nucleoli. This may indicate that the nucleolus act as a storage compartment for hENDOV isoform 1. Since this was only observed after exposure of the CPT and not the other agents (MMS, MMC, and gamma radiation) it is difficult to draw an absolute conclusion. As this system is based on overexpression, one cannot exclude that the other agent also results in relocalisation of parts of the fusion protein that is match by the high expression level.

Camptothecin is a secondary metabolite used as an anti-cancer drug that damages DNA, leading to the destruction of the cell. Camptothecin affects the activity of the enzyme topoisomerase I, whose normal action is alleviate supercoiling in DNA by cleaving, unwinding, and religate of the DNA. When camptothecin binds topoisomerase I, the enzyme will be able to cleave but not religate DNA. Thereby, camptothecin causes double-strand breaks in DNA (Buckwalter et al. 1996;Rubbi and Milner 2003). For the topoisomerase I-targeted drug camptothecin, lethal DNA damage has been proposed to occur as a result of the interaction of the DNA replication apparatus with the drug-trapped enzyme-DNA complex (Nelson and Kastan 1994).

The role of hENDOV in the nucleoli remains unclear. The primary role of this subnuclear compartment is in ribosome biogenesis, although emerging evidence suggests additional non-ribosomal functions (Raska *et al.* 2006;Boisvert *et al.* 2007). Many proteins, including DNA repair proteins, have been shown to localize to the nucleoli. For some, like the RecQ helicases WRN and BLM, the nucleolus seems to be sequestering compartment since the proteins were recruited to distinct nuclear foci when cells were exposed to certain damaging agents (Marciniak *et al.* 1998;Yankiwski *et al.* 2000;Sanz *et al.* 2000;Karmakar and Bohr 2005;Otterlei *et al.* 2006). In marked contrast, the RECQL4 helicase did not relocate after treatment with various DNA damaging agents, but the protein accumulated in the nucleoli upon oxidative stress (Woo et al. 2006). Thus, the nucleolar localization clearly serves different functions for different proteins.

Nucleolar proteins like nucleolin and topoisomerase I have been describing underwent p53-dependent relocalisation from nucleoli after cellular stress such as heat shock and DNA damage, respectively (Mao *et al.* 2002;Daniely *et al.* 2002). HeLa cells, utilized in our study, are cancerous cells defective in p53, a protein involved in the DNA damage response and malfunctioning in several cancer cells. Cell lines with functional p53 protein should, therefore, be employed in further studies to elucidate the role of hENDOV in nucleoli.

5.3.1 Methodological aspects

To examine the intracellular localisation of the three isoforms hENDOV that was used in this study, we overexpressed EGFP-tagged protein in HeLa-S3 cells. When evaluating the result we therefore need to consider the use of a tagged protein which is present in excess amounts in the cells. Overexpression of proteins in cells may generate novel phenotypes. Increased amounts of protein can also lead to disrupted intracellular protein localisation, in addition to possibilities for masking relocalisation of the protein. We observed that the nucleoli localization was changed for hENDOV isoform 1 hour CPT treatment. Another problem arising when studying overexpressed proteins is that the unnatural amount of protein will introduce an unbalanced environment in respect to protein interactions and cellular response involving other proteins.

One advantage with tagged proteins is that they can be studied in living cells evading the artefacts of cell fixation and permeabilisation. However, GFP is a 27 kDa protein which may affect the localisation of the attached protein. New technologies are under way to solve these problems, of which the use of small arsenical based fluorescent compounds is one example (Griffin et al. 1998).

In this period of work I have devoted a lot of time on developing and testing antibodies towards human ENDOV and mouse EndoV without much success. This is a common problem in the DNA repair field in respect to antibodies recognising specific proteins. Several report on e.g. OGG1 immunocytochemistry have been published, although, a growing scepticism towards the specificity of the antibodies is apparent. The level of DNA glycosylases in cells have been proposed to be too low to be detected with antibodies, which may also apply to endonuclease V.

5.4 MTT-assay

In this study we used a viability assay (MTT-assay) to determine the ability of MEF cells to maintain or recover its viability after CPT exposure and treatment with other DNA damaging agents. An important step in transformation is immortalization, in which cells gain the ability to grow indefinitely by bypassing cellular senescence that imposes a finite number of divisions in culture. Primary mouse embryonic fibroblast (MEF) cells have limited growth capacity and on prolonged passing spontaneously immortalize at a low frequency (Sun and Taneja 2007). In this study we have worked with constitutive knockout mouse, *mEndoV* +/+ (WT) and *mEndo* -/- (KO). Others in the laboratory have isolated mouse embryonic fibroblast cells and with prolonged passaging spontaneously transformed the MEF cells used in this thesis.

No cytotoxic effects were obtained between MEF WT and KO cell lines after CPT exposure or treatment with other DNA damaging agents. We started to look at early transformed MEF cells, these lines showed a substantial variation in survival between isogenic isolates. Because of this, we decided to perform the MTT-assay on the corresponding primary MEF lines. These lines have not been spontaneously transformed, which could eliminate the variation within these cell lines. This variation was eliminated using primary MEF cell lines, but no cytotoxic effects were observed between the WT and KO after treatment with DNA damaging agents. Both WT and KO had a representable dose response to CPT and to the other agents, as shown in the results. Based on these observations, we can conclude that we found no effect of knocking out the gene for *EndoV* and exposing the cells for DNA damaging agents. This supports the theory that eukaryotic EndoV can have a different role than prokaryotic EndoV.

5.5 Constitutive or conditional knockout

In this study a *mEndoV* constitutive knockout mouse was made over a conditional knockout (made by Professor A. Klungland's group at the same department). Both variants have drawbacks. Constructing a conditional knockout mouse is more laborious, more time-consuming and is more expensive to produce than a constitutive knockout. The major drawback with the constitutive knockout is that if removal of the gene of interest, in our case *mEndoV*, leads to embryonic lethality this precludes the analysis of a potential adult phenotype. Other undesirable effects of the gene inactivation can be pleiotropic side effects. These are compensatory reactions to the introduced germ line mutation obscuring or preventing a clear-cut analysis. Moreover, the knocked out gene may have a function during early development and its invalidation might induce a highly complicated accumulative phenotype which does not necessarily represent solely the gene of interest (Bockamp et al. 2002).

Analysing the gene function at a specific developmental window or in a particular cell lineage might be necessary. In a constitutive knockout the targeted gene is inactivated in all cells from birth until death, whereas conditional knockout allows the spatiotemporal control of the gene silencing. Therefore, knockout can prevent unwanted pleiotropic side effects and exclude accumulative compensatory developmental changes from the earliest embryonic stages.

5.6 Final conclusions and future work

We are familiar with that the fact there is a high (and uncertain) number of isoforms of human ENDOV, which makes it difficult to characterize and determine the function of this protein. The RACE experiments gave no special clarifications of the *hENDOV* transcripts. This may be due to bad quality of the cDNA obtained from Clontech, since we saw that the adaptor was inserted in exon 8 in the 3'RACE experiments. The Real-Time qPCR technique can be used to quantify the amount of the total level of *hENDOV* transcripts in normal cells, which can provide a better clarification of the different *hENDOV* transcripts. The full-length *hENDOV* transcript (exon 3-contaning) does not represent the majority of the transcripts variants in the human cells.

The three different transcript variants of human *hENDOV* were successfully subcloned and expressed in fusion with green fluorescent protein (GFP). The purified recombinant hENDOV FL was used to produce an antibody against human ENDOV by immunization of rabbits.

We showed that hENDOV isoform 1 was located to the cytoplasm and nucleus with enrichment in nucleoli. But the other two isoforms showed only localization in the cytoplasm. These isoforms may reflect different roles of human ENDOV, such as different substrates, cellular localization, cell-cycle dependent or organ-specific forms. There is a particular interest in the hENDOV isoform 2 (lacking exon 3), which that lacks central parts of the DNA binding and catalytic regions. Work is in progress to optimize the protein purification protocol for this from.

E. coli EndoV is known to bind to the DNA, and similar studies have been performed with human ENDOV. These binding studies (done by other people in the laboratory) showed hENDOV isoform 1 specifically bound to 3'flap, 5'flap, fork, pseudo-Y, 3-way junction, and 4-way junction (Holliday junction) DNA. No binding was observed for inosine or A:TT loop DNA. This demonstrates that if hENDOV is involved in DNA repair in human cells, it would be differently than *E. coli* EndoV, of which inosine is the main substrate. hENDOV is shown to bind specifically to Holliday junction DNA, suggesting that it is involved in genetic recombination, such as a Holliday junction resolvase. This hypothesis is further supported by structural studies that show that prokaryotic ENDOV contain RNaseH-like motif similar to the Holliday junction resolvase RuvC. Multiple sequence analyses show that ENDOV is

highly conserved from prokaryotes to humans, and it is thus likely that hENDOV also contains the RNase H-like motif.

E. coli EndoV recognizes certain DNA damages and nicks the DNA strand 3' of the lesion. hENDOV was also tested in our laboratory for endonucleolytic activity. No activity was found for 5'flap, 3-way junction, or 4-way junction DNA. Several different buffers were used, exploring different pH and metal ion condition. Bioinformatics confirm the conservation of ENDOV's catalytic residue from *E. coli* to *Homo sapiens,* and it is thus surprising that no endonucleolytic activity for hENDOV has been discovered.

Regarding the biochemistry of human ENDOV, optimization of the DNA binding protocol and extension of the enzymatic assay should be explored to reveal possible endonucleolytic activity. In these experiments, possible protein partners and sequence specific DNA substrates should also be tested. Another way to identify protein partners or the pathway of ENDOV is by mapping of genetic interactions by double-mutant knockout experiment. Such analyses are most conveniently carried out using simpler model organisms like *E. coli* or yeast (*S. pombe* or *S. cerevisiae)* for prokaryotes and eukaryotes, respectively.

In summary, this thesis presents the first results of the characterization of the human ENDOV protein, which is highly conserved in all domains of life, yet probably with different roles in prokaryotic and eukaryotic cells.

References

Aas, P. A., Otterlei, M., Falnes, P. Ø., Vågbø, C. B., Skorpen, F., Akbari, M., Sundheim, O., Bjørås, M., Slupphaug, G., Seeberg, E., & Krokan, H. E. (2003). Human and bacterial oxidative demethylases repair alkylation damage in both RNA and DNA, *Nature*, vol. 421, no. 6925, pp. 859-863.

Alberts, B., Johnson, A., Lewis, J., Raff, M., Roberts, K., & Walter, P. (2008). Molecular biology of the cell, 5th ed, Garland Science, New York, pp. 36-42.

Altieri, F., Grillo, C., Maceroni, M., & Chichiarelli, S. (2008). DNA damage and repair: from molecular mechanisms to health implications, *Antioxidants & Redox Signaling*, vol. 10, no. 5, pp. 891-938.

Aravind, L., Walker, D. R., & Koonin, E. V. (1999). Conserved domains in DNA repair proteins and evolution of repair systems, *Nucleic Acids Research*, vol. 27, no. 5, pp. 1223-1242.

Balajee, A. S. & Bohr, V. A. (2000). Genomic heterogeneity of nucleotide excision repair, *Gene*, vol. 250, no. 1-2, pp. 15-30.

Barnes, D. E. & Lindahl, T. (2004). Repair and genetic consequences of endogenous DNA base damage in mammalian cells, *Annu.Rev.Genet.*, vol. 38, pp. 445-476.

Barrows, L. P. & Magee, P. N. (1982). Nonenzymatic methylation of DNA by S-adenosylmethionine in-vitro, *Carcinogenesis (Oxford)*, vol. 3, no. 3, pp. 349-352.

Bockamp, E., Maringer, M., Spangenberg, C., Fees, S., Fraser, S., Eshkind, L., Oesch, F., & Zabel, B. (2002).Of mice and models: improved animal models for biomedical research", *Physiological Genomics*, vol. 11, no. 3, pp. 115-132.

Bohm, C., Seibel, N. M., Henkel, B., Steiner, H., Haass, C., & Hampe, W. (2006). SorLA signaling by regulated intramembrane proteolysis", *Journal of Biological Chemistry*, vol. 281, no. 21, pp. 14547-14553.

Boisvert, F.-M., van Koningsbruggen, S., Navascués, J., & Lamond, A. I. (2007). The multifunctional nucleolus, *Nature reviews Molecular cell biology*, vol. 8, no. 7, pp. 574-585.

Brem, R. & Hall, J. (2005). XRCC1 is required for DNA single-strand break repair in human cells, *Nucleic Acids Research*, vol. 33, no. 8, pp. 2512-2520.

Brookes, P. & Lawley, P. D. (1964). Alkylating agents, *British Medical Bulletin*, vol. 20, no. 2, p. 91-&.

Buckwalter, C. A., Lin, A. H., Tanizawa, A., Pommier, Y. G., Cheng, Y. C., & Kaufmann, S. H. (1996). RNA synthesis inhibitors alter the subnuclear distribution of DNA topoisomerase I, *Cancer research*, vol. 56, no. 7, pp. 1674-1681.

Burney, S., Caulfield, J. L., Niles, J. C., Wishnok, J. S., & Tannenbaum, S. R. (1999). The chemistry of DNA damage from nitric oxide and peroxynitrite, *Mutation Research/Fundamental and Molecular Mechanisms of Mutagenesis*, vol. 424, no. 1-2, pp. 37-49.

Cahill, D., Connor, B., & Carney, J. P. (2006). Mechanisms of eukaryotic DNA double strand break repair, *Frontiers in Bioscience*, vol. 11, pp. 1958-1976.

Chan, W., Costantino, N., Li, R., Lee, S. C., Su, Q., Melvin, D., Court, D., & Liu, P. (2007). A recombineering based approach for high-throughput conditional knockout targeting vector construction, *Nucleic Acids Research*, vol. 35, no. 8.

Christmann, M., Tomicic, M. T., Roos, W. P., & Kaina, B. (2003). Mechanisms of human DNA repair: an update, *Toxicology*, vol. 193, no. 1-2, pp. 3-34.

Dalhus, B., Laerdahl, J. K., Backe, P. H., & Bjørås, M. (2009). DNA base repair - recognition and initiation of catalysis, *FEMS Microbiology Reviews*, vol. 33, no. 6, pp. 1044-1078.

Daniely, Y., Dimitrova, D. D., & Borowiec, J. A. (2002). Stress-dependent nucleolin mobilization mediated by p53-nucleolin complex formation, *Molecular and Cellular Biology*, vol. 22, no. 16, pp. 6014-6022.

Dao, V. & Modrich, P. (1998). Mismatch-, MutS-, MutL-, and helicase II-dependent unwinding from the single-strand break of an incised heteroduplex, *Journal of Biological Chemistry*, vol. 273, no. 15, pp. 9202-9207.

Drabløs, F., Feyzi, E., Aas, P. A., Vaagbø, C. B., Kavli, B., Bratlie, M. S., Peña-Diaz, J., Otterlei, M., Slupphaug, G., & Krokan, H. E. (2004). Alkylation damage in DNA and RNA—repair mechanisms and medical significance, *DNA repair*, vol. 3, no. 11, pp. 1389-1407.

Falnes, P. Ø., Johansen, R. F., & Seeberg, E. (2002). AlkB-mediated oxidative demethylation reverses DNA damage in Escherichia coli, *Nature*, vol. 419, no. 6903, pp. 178-182.

Feng, H., Klutz, A. M., & Cao, W. (2005). Active site plasticity of endonuclease V from Salmonella typhimurium, *Biochemistry*, vol. 44, no. 2, pp. 675-683.

Fields, S. & Johnston, M. (2005). Whither model organism research?, *Science*, vol. 307, no. 5717, p. 1885.

Fishel, R., Lescoe, M. K., Rao, M. R., Copeland, N. G., Jenkins, N. A., Garber, J., Kane, M., & Kolodner, R. (1994). The human mutator gene homolog MSH2 and its association with hereditary nonpolyposis colon cancer, *Cell.*, vol. 77, no. 1.

Fishel, R. & Kolodner, R. D. (1995). Identification of mismatch repair genes and their role in the development of cancer, *Current Opinion in Genetics & Development*, vol. 5, no. 3, pp. 382-395.

Fitzgerald-Hayes, M. & Reichsman, F. (2010). DNA and biotechnology," 3rd ed, Elsevier/Academic Press, Burlington, Mass, pp. 5-7.

Fortini, P., Pascucci, B., Parlanti, E., D'Errico, M., Simonelli, V., & Dogliotti, E. (2003). The base excision repair: mechanisms and its relevance for cancer susceptibility, *Biochimie*, vol. 85, no. 11, pp. 1053-1071.

Fortini, P., Pascucci, B., Parlanti, E., Sobol, R. W., Wilson, S. H., & Dogliotti, E. (1998). Different DNA polymerases are involved in the short- and long-patch base excision repair in mammalian cells, *Biochemistry*, vol. 37, no. 11, pp. 3575-3580.

Friedberg, E. C. (2003). DNA damage and repair, *Nature*, vol. 421, no. 6921, pp. 436-440.

Friedberg, E. C., Walker, G. C., Siede, W., Wood, R. A., Schultz, R. A., & Ellenberger, T. (2006). *DNA repair and mutagenesis*, 2nd edn, ASM Press, Washington, D.C.

Gates, F. T. & Linn, S. (1977). Endonuclease V of Escherichia coli, *Journal of Biological Chemistry*, vol. 252, no. 5, p. 1647.

Griffin, B. A., Adams, S. R., & Tsien, R. Y. (1998). Specific Covalent Labeling of Recombinant Protein Molecules Inside Live Cells, *Science*, vol. 281, no. 5374, pp. 269-272.

Gros, L., Ishchenko, A. A., Ide, H., Elder, R. H., & Saparbaev, M. K. (2004). The major human AP endonuclease (Ape1) is involved in the nucleotide incision repair pathway, *Nucleic Acids Research*, vol. 32, no. 1, pp. 73-81.

Guo, G., Ding, Y., & Weiss, B. (1997). nfi, the gene for endonuclease V in Escherichia coli K-12, *Journal of bacteriology*, vol. 179, no. 2, p. 310.

Hadjiolov, A. A. (1985), *The nucleolus and ribosome biogenesis* Springer-Verlag, Wien, vol. 12

Hakem, R. (2008). DNA-damage repair; the good, the bad, and the ugly, *The EMBO journal*, vol. 27, no. 4, pp. 589-605.

Hansen, W. K. & Kelley, M. R. (2000). Review of mammalian DNA repair and translational implications, *Journal of Pharmacology and Experimental Therapeutics*, vol. 295, no. 1, pp. 1-9.

He, B., Qing, H., & Kow, Y. W. (2000). Deoxyxanthosine in DNA is repaired by Escherichia coli endonuclease V, *Mutation Research*, vol. 459, no. 2, pp. 109-114.

Hoeijmakers, J. H. J. (2001). Genome maintenance mechanisms for preventing cancer, *Nature*, vol. 411, no. 6835, pp. 366-374.

Hoeijmakers, J. H. J. (2009). DNA damage, aging, and cancer, *New England Journal of Medicine*, vol. 361, no. 15, pp. 1475-1485.

Huang, J., Lu, J., Barany, F., & Cao, W. (2001). Multiple cleavage activities of endonuclease V from Thermotoga maritima: Recognition and strand nicking mechanism, *Biochemistry*, vol. 40, no. 30, pp. 8738-8748.

Ischenko, A. A. & Saparbaev, M. K. (2002). Alternative nucleotide incision repair pathway for oxidative DNA damage, *Nature*, vol. 415, no. 6868, pp. 183-187.

Ishchenko, A. A., Sanz, G. l., Privezentzev, C. V., Maksimenko, A. V., & Saparbaev, M. (2003). Characterisation of new substrate specificities of Escherichia coli and Saccharomyces cerevisiae AP endonucleases, *Nucleic Acids Research*, vol. 31, no. 21, pp. 6344-6353.

Izumi, T., Wiederhold, L. R., Roy, G., Roy, R., Jaiswal, A., Bhakat, K. K., Mitra, S., & Hazra, T. K. (2003). Mammalian DNA base excision repair proteins: their interactions and role in repair of oxidative DNA damage, *Toxicology*, vol. 193, no. 1-2, pp. 43-65.

Karmakar, P. & Bohr, V. A. (2005). Cellular dynamics and modulation of WRN protein is DNA damage specific, *Mechanisms of Ageing and Development*, vol. 126, no. 11, pp. 1146-1158.

Karran, P. (2000). DNA double strand break repair in mammalian cells, *Current Opinion in Genetics & Development*, vol. 10, no. 2, pp. 144-150.

Kirouac, K. N. & Ling, H. (2011). Unique active site promotes error-free replication opposite an 8-oxo-guanine lesion by human DNA polymerase iota, *Proceedings of the National Academy of Sciences*, vol. 108, no. 8, p. 3210.

Klungland, A. (2001). Et liv uten DNA-reparasjon, *Tidsskrift for den Norske Lægeforening*, vol. 121, no. 1.

Klungland, A. & Lindahl, T. (1997). Second pathway for completion of human DNA base excision-repair: reconstitution with purified proteins and requirement for DNase IV (FEN1), *The EMBO journal*, vol. 16, no. 11, pp. 3341-3348.

Kow, Y. W. (1999). Oxidative stress, DNA damage and human diseases, *Dojindo Newsletter*, vol. 2, pp. 4-13.

Kow, Y. W. (2002). Repair of deaminated bases in DNA, *Free Radical Biology and Medicine*, vol. 33, no. 7, pp. 886-893.

Krokan, H. E., Kavli, B., & Slupphaug, G. (2004). Novel aspects of macromolecular repair and relationship to human disease, *Journal of Molecular Medicine*, vol. 82, no. 5, pp. 280-297.

Kubota, Y., Nash, R. A., Klungland, A., Schär, P., Barnes, D. E., & Lindahl, T. (1996). Reconstitution of DNA base excision-repair with purified human proteins: interaction between DNA polymerase beta and the XRCC1 protein, *The EMBO journal*, vol. 15, no. 23, pp. 6662-6670.

Kunkel, T. A. & Erie, D. A. (2005). DNA mismatch repair, *Annual review of biochemistry*, vol. 74, pp. 681-710.

Kurowski, M. A., Bhagwat, A. S., Papaj, G., & Bujnicki, J. M. (2003). Phylogenomic identification of five new human homologs of the DNA repair enzyme AlkB, *BMC Genomics*, vol. 4, no. 1.

Lahue, R. S., Au, K. G., & Modrich, P. (1989). DNA mismatch correction in a defined system, *Science (New York, N.Y.)*, vol. 245, no. 4914, pp. 160-164.

Leach, F. S., Nicolaides, N. C., Papadopoulos, N., Liu, B., Jen, J., Parsons, R., Peltomaki, P., Sistonen, P., Aaltonen, L. A., Nystrom-Lahti, M., Guan, X. Y., Zhang, J., Meltzer, P. S., Yu, J. W., Kao, F. T., Chen, D. J., Cerosaletti, K. M., Fournier, R. E. K., Todd, S., Lewis, T., Leach, R. J., Naylor, S. L., Weissenbach, J., Mecklin, J. P., Jarvinen, H., Petersen, G. M., Hamilton, S. R., Green, J., Jass, J., Watson, P., Lynch, H. T., Trent, J. M., Chapelle, A. d. l., Kinzler, K. W., & Vogelstein, B. (1993). Mutations of a mutS Homolog in Hereditary Nonpolyposis Colorectal Cancer, *Cell.*, vol. 75, no. 6.

Lee, Y. & McKinnon, P. J. (2007). Responding to DNA double strand breaks in the nervous system, *Neuroscience*, vol. 145, no. 4, pp. 1365-1374.

Lehmann, A. R. (2001). The xeroderma pigmentosum group D (XPD) gene: One gene, two functions, three diseases, *Genes and Development*, vol. 15, no. 1, pp. 15-23.

Li, G. M. (2008). Mechanisms and functions of DNA mismatch repair, *Cell research*, vol. 18, no. 1, pp. 85-98.

Lindahl, T. (1974). An N-glycosidase from Escherichia coli that releases free uracil from DNA containing deaminated cytosine residues, *Proceedings of the National Academy of Sciences*, vol. 71, no. 9, p. 3649.

Lindahl, T. (1993). Instability and decay of the primary structure of DNA, *Nature*, vol. 362, no. 6422, p. 709.

Lindahl, T. & Barnes, D. E. (2000). Repair of endogenous DNA damage, *Cold Spring Harbor symposia on quantitative biology.*, vol. 65, pp. 127-133.

Lindahl, T. & Karlstro, O. (1973). Heat-induced depyrimination of deoxyribonucleic acid in neutral solution, *Biochemistry*, vol. 12, no. 25, pp. 5151-5154.

Liu, L., Xu-Welliver, M., Kanugula, S., & Pegg, A. E. (2002). Inactivation and degradation of O6-alkylguanine-DNA alkyltransferase after reaction with nitric oxide, *Cancer research*, vol. 62, no. 11, pp. 3037-3043.

Lundin, C., North, M., Erixon, K., Walters, K., Jenssen, D., Goldman, A. S. H., & Helleday, T. (2005). Methyl methanesulfonate (MMS) produces heat-labile DNA damage but no detectable in vivo DNA double-strand breaks, *Nucleic Acids Research*, vol. 33, no. 12, pp. 3799-3811.

Mao, Y., Mehl, I. R., & Muller, M. T. (2002). Subnuclear distribution of topoisomerase I is linked to ongoing transcription and p53 status, *Proceedings of the National Academy of Sciences of the United States of America*, vol. 99, no. 3, pp. 1235-1240.

Marciniak, R. A., Lombard, D. B., Johnson, F. B., & Guarente, L. (1998). Nucleolar localization of the Werner syndrome protein in human cells, *Proceedings of the National Academy of Sciences of the United States of America*, vol. 95, no. 12, pp. 6887-6892.

Maynard, S., Schurman, S. H., Harboe, C., de Souza-Pinto, N. C., & Bohr, V. A. (2009). Base excision repair of oxidative DNA damage and association with cancer and aging, *Carcinogenesis (Oxford)*, vol. 30, no. 1, p. 2.

Mellon, I. (2005). Transcription-coupled repair: A complex affair", *Mutation Research Regular Papers*, vol. 577, no. 1-2, pp. 155-161.

Mellon, I., Spivak, G., & Hanawalt, P. C. (1987). Selective removal of transcription-blocking DNA damage from the transcribed strand of the mammalian DHFR gene, *Cell.*, vol. 51, no. 2, pp. 241-249.

Mishina, Y., Duguid, E. M., & He, C. (2006), "Direct reversal of DNA alkylation damage", *Chemical Reviews*, vol. 106, no. 2, pp. 215-232.

Moe, A., Ringvoll, J., Nordstrand, L. M., Eide, L., Bjørås, M., Seeberg, E., Rognes, T., & Klungland, A. (2003). Incision at hypoxanthine residues in DNA by a mammalian homologue of the Escherichia coli antimutator enzyme endonuclease V, *Nucleic Acids Research*, vol. 31, no. 14, pp. 3893-3900.

Moore, J. K. & Haber, J. E. (1996). Cell cycle and genetic requirements of two pathways of nonhomologous end-joining repair of double-strand breaks in Saccharomyces cerevisiae, *Molecular and Cellular Biology*, vol. 16, no. 5, pp. 2164-2173.

Naslund, M., Segerback, D., & Kolman, A. (1983). S-Adenosylmethionine, an endogenous alkylating agent., *Mutation Research*, vol. 119, no. 3-4, pp. 229-232.

Nelson, W. G. & Kastan, M. B. (1994). DNA strand breaks: the DNA template alterations that trigger p53-dependent DNA damage response pathways, *Molecular and Cellular Biology*, vol. 14, no. 3, pp. 1815-1823.

Nilsen, H. & Krokan, H. E. (2001). Base excision repair in a network of defence and tolerance, *Carcinogenesis (Oxford)*, vol. 22, no. 7, pp. 987-998.

Nowosielska, A. & Marinus, M. G. (2008). DNA mismatch repair-induced double-strand breaks, *DNA repair*, vol. 7, no. 1, pp. 48-56.

Nyberg, K. A., Michelson, R. J., Putnam, C. W., & Weinert, T. A. (2002). Toward maintaining the genome: DNA damage and replication checkpoints, *Annual review of genetics*, vol. 36, no. 1, pp. 617-656.

Ogi, T., Limsirichaikul, S., Overmeer, R. M., Volker, M., Takenaka, K., Cloney, R., Nakazawa, Y., Niimi, A., Miki, Y., Jaspers, N. G., Mullenders, L. H. F., Yamashita, S., Fousteri, M. I., & Lehmann, A. R. (2010). Three DNA Polymerases, Recruited by Different Mechanisms, Carry Out NER Repair Synthesis in Human Cells, *Molecular Cell*, vol. 37, no. 5, pp. 714-727.

Otterlei, M., Bruheim, P., Ahn, B., Bussen, W., Karmakar, P., Baynton, K., & Bohr, V. A. (2006). Werner syndrome protein participates in a complex with RAD51, RAD54, RAD54B and ATR in response to ICL-induced replication arrest, *Journal of cell science*, vol. 119, no. 24, pp. 5137-5146.

Pennacchio, L. A. (2003). Insights from human/mouse genome comparisons, *Mammalian Genome*, vol. 14, no. 7, pp. 429-436.

Plumb, J. A. (2004). Cell sensitivity assays: the MTT assay, *Methods in molecular medicine*, vol. 88, pp. 165-170.

Prasad, R., Dianov, G. L., Bohr, V. A., & Wilson, S. H. (2000). FEN1 stimulation of DNA polymerase beta mediates an excision step in mammalian long patch base excision repair, *Journal of Biological Chemistry*, vol. 275, no. 6, pp. 4460-4466.

Qiagen® (2005). Qiagen® Plasmid Purification Handbook, 3rd edn, pp. 19-23.

Rannug, U. L. F., Göthe, R., & Wachtmeister, C. A. (1976). The mutagenicity of chloroethylene oxide, chloroacetaldehyde, 2-chloroethanol and chloroacetic acid, conceivable metabolites of vinyl chloride, *Chemico-Biological Interactions*, vol. 12, no. 3-4, pp. 251-263.

Raska, I., Shaw, P. J., & Cmarko, D. (2006). New insights into nucleolar architecture and activity, *International review of Cytology - A Survey of cell Biology*, vol. 255, pp. 177-235.

Reardon, J. T. & Sancar, A. (2005). Nucleotide excision repair, *Progress in Nucleic acid Research and Molecular biology*, vol. 79, pp. 183-235.

Ringvoll, J., Nordstrand, L. M., Vågbø, C. B., Talstad, V., Reite, K., Aas, P. A., Lauritzen, K. H., Liabakk, N. B., Bjørk, A., Doughty, R. W., Falnes, P. Ø., Krokan, H. E., & Klungland, A. (2006). Repair deficient mice reveal mABH2 as the primary oxidative demethylase for repairing 1meA and 3meC lesions in DNA", *The EMBO journal*, vol. 25, no. 10, pp. 2189-2198.

Rubbi, C. P. & Milner, J. (2003). Disruption of the nucleolus mediates stabilization of p53 in response to DNA damage and other stresses, *The EMBO journal*, vol.22 , pp. 6068-6077.

Rydberg, B. & Lindahl, T. (1982). Nonenzymatic methylation of DNA by the intracellular methyl group donor S-adenosyl-L-methionine is a potentially mutagenic reaction, *The EMBO journal*, vol. 1, no. 2, pp. 211-216.

Sancar, A., Lindsey-Boltz, L. A., Unsal-Ka+ºmaz, K., & Linn, S. (2004). Molecular mechanisms of mammalian DNA repair and the DNA damage checkpoints, *Annual review of biochemistry.*, vol. 73, pp. 39-85.

Sancar, G. B. (1990). DNA photolyases: physical properties, action mechanism, and roles in dark repair, *Mutation research.*, vol. 236, no. 2-3, pp. 147-160.

Sanz, M. M., Proytcheva, M., Ellis, N. A., Holloman, W. K., & German, J. (2000). BLM, the Bloom`s syndrome protein, varies during the cell cycle in its amount, distribution, and co-localization with other nuclear proteins, *Cytogenetics and Cell Genetics*, vol. 91, no. 1ΓÇô4, pp. 217-223.

Saparbaev, M. & Laval, J. (1994). Excision of hypoxanthine from DNA containing dIMP residues by the Escherichia coli, yeast, rat, and human alkylpurine DNA glycosylases, *Proceedings of the National Academy of Sciences of the United States of America*, vol. 91, no. 13, pp. 5873-5877.

Schouten, K. A. & Weiss, B. (1999). Endonuclease V protects Escherichia coli against specific mutations caused by nitrous acid, *Mutation Research/DNA Repair*, vol. 435, no. 3, pp. 245-254.

Sedgwick, B., Bates, P. A., Paik, J., Jacobs, S. C., & Lindahl, T. (2007). Repair of alkylated DNA: recent advances, *DNA repair*, vol. 6, no. 4, pp. 429-442.

Sedgwick, B. (2004). Repairing DNA-methylation damage, *Nature reviews Molecular cell biology*, vol. 5, no. 2, pp. 148-157.

Seeberg, E., Nissen-Meyer, J., & Strike, P. (1976), Incision of ultraviolet-irradiated DNA by extracts of E. coli requires three different gene products, *Nature*, vol. 263, no. 5577, pp. 524-526.

Shapiro, R. & Shiuey, S. J. (1969). Reaction of nitrous acid with alkylaminopurines, *Biochimica et biophysica acta*, vol. 174, no. 1, p. 403.

Slupphaug, G., Kavli, B., & Krokan, H. E. (2003). The interacting pathways for prevention and repair of oxidative DNA damage, *Mutation Research/Fundamental and Molecular Mechanisms of Mutagenesis*, vol. 531, no. 1-2, pp. 231-251.

Stucki, M., Pascucci, B., Parlanti, E., Fortini, P., Wilson, S. H.,Hübscher, U., & Dogliotti, E. (1998). Mammalian base excision repair by DNA polymerases delta and epsilon, *Oncogene*, vol. 17, no. 7, pp. 835-843.

Sun, H. & Taneja, R. (2007). Analysis of transformation and tumorigenicity using mouse embryonic fibroblast cells, *Methods in molecular biology.*, vol. 383, pp. 303-310.

Sung, P. & Klein, H. (2006). Mechanism of homologous recombination: mediators and helicases take on regulatory functions, *Nature reviews Molecular cell biology*, vol. 7, no. 10, pp. 739-750.

Sylvester, P. W. (2011). Optimization of the tetrazolium dye (MTT) colorimetric assay for cellular growth and viability, *Methods in molecular biology.*, vol. 716, pp. 157-168.

Thompson, L. H. & Schild, D. (2002). Recombinational DNA repair and human disease, *Mutation Research/Fundamental and Molecular Mechanisms of Mutagenesis*, vol. 509, no. 1-2, pp. 49-78.

Thoms, K. M., Kuschal, C., & Emmert, S. (2007). Lessons learned from DNA repair defective syndromes, *Experimental dermatology*, vol. 16, no. 6, pp. 532-544.

Todo, T. (1999). Functional diversity of the DNA photolyase/blue light receptor family, *Mutation Research*, vol. 434, no. 2, pp. 89-97.

Trewick, S. C., Henshaw, T. F., Hausinger, R. P., Lindahl, T., & Sedgwick, B. (2002). Oxidative demethylation by Escherichia coli AlkB directly reverts DNA base damage", *Nature*, vol. 419, no. 6903, pp. 174-178.

Tsien, R. Y. (1998). The green fluorescent protein, *Annual review of biochemistry*, vol. 67, no. 1, pp. 509-544.

Vermeulen, W., De Boer, J., Citterio, E., Van Gool, A. J., Van Der Horst, G. T. J., Jaspers, G. J., De Laat, W. L., Sijbers, A. M., Van Der Spek, P. J., Sugasawa, K., Weeda, G., Winkler, G. S., Boostma, D., Egly, J. M., & Hoeijmakers, J. H. J. (1997). Mammalian nucleotide excision repair and syndromes, *Biochemical Society Transactions*, vol. 25, no. 1, pp. 309-315.

Weiss, B. (2008). Removal of deoxyinosine from the Escherichia coli chromosome as studied by oligonucleotide transformation, *DNA repair*, vol. 7, no. 2, pp. 205-212.

Woo, L. L., Futami, K., Shimamoto, A., Furuichi, Y., & Frank, K. M. (2006). The Rothmund-Thomson gene product RECQL4 localizes to the nucleolus in response to oxidative stress, *Experimental Cell Research*, vol. 312, no. 17, pp. 3443-3457.

Wood, R. D., Mitchell, M., & Lindahl, T. (2005). Human DNA repair genes, *Mutat.Res.*, vol. 577, no. 1-2, pp. 275-283.

Yang, W. (2000). Structure and function of mismatch repair proteins, *Mutation Research*, vol. 460, no. 3-4, pp. 245-256.

Yankiwski, V., Marciniak, R. A., Guarente, L., & Neff, N. F. (2000). Nuclear structure in normal and Bloom syndrome cells, *Proceedings of the National Academy of Sciences of the United States of America*, vol. 97, no. 10, pp. 5214-5219.

Yao, M., Hatahet, Z., Melamede, R. J., & Kow, Y. W. (1994). Purification and characterization of a novel deoxyinosine-specific enzyme, deoxyinosine 3' endonuclease, from Escherichia coli, *Journal of Biological Chemistry*, vol. 269, no. 23, pp. 16260-16268.

Yao, M. & Kow, Y. W. (1996). Cleavage of insertion/deletion mismatches, flap and pseudo-Y DNA structures by deoxyinosine 3'-endonuclease from Escherichia coli, *Journal of Biological Chemistry*, vol. 271, no. 48, pp. 30672-30676.

Yao, M. & Wah-Kow, Y. (1997). Further characterization of Escherichia coli endonuclease V: Mechanism of recognition for deoxyinosine, deoxyuridine, and base mismatches in DNA, *Journal of Biological Chemistry*, vol. 272, no. 49, pp. 30774-30779.

Appendix I: NCBI Reference sequence (*hENDOV*)

Homo sapiens endonuclease V transcript variant 1, mRNA

NCBI Reference Sequence: NM_173627.3

With exon 3 and short exon 9 + exon 10

>gi|257467546|ref|NM_173627.3| Homo sapiens endonuclease V (ENDOV), transcript variant 1, mRNA

GTGCGGAAGGGGTGCCCGGGACGAAGCC**ATG**GCCCTGGAGGCGGCGGGAGGGCCGCCGGAGG
AAACGCTGTCACTGTGGAAACGGGAGCAAGCTCGGCTGAAGGCCCACGTCGTAGACCGGGAC
ACCGAGGCGTGGCAGCGAGACCCCGCCTTCTCGGGTCTGCAGAGGGTCGGGGGCGTTGACGT
GTCCTTCGTGAAAGGGGACAGTGTCCGCGCTTGTGCTTCCCTGGTGGTGCTCAGCTTCCCTG
AGCTCGAGGTGGTGTATGAGGAGAGCCGCATGGTCAGCCTCACAGCCCCCTACGTGTCGGGC
TTCCTGGCCTTCCGAGAGGTGCCCTTCTTGCTGGAGCTGGTGCAGCAGCTGCGGGAGAAGGA
GCCGGGCCTCATGCCCCAGGTCCTTCTTGTGGATGGAAACGGGGTACTCCACCACCGAGGCT
TTGGGGTGGCCTGCCACCTTGGCGTCCTTACAGACCTGCCGTGTGTTGGGGTGGCCAAGAAA
CTTCTGCAGGTGGATGGGCTGGAGAACAACGCCCTGCACAAGGAGAAGATCCGACTCCTGCA
GACTCGAGGAGACTCATTCCCTCTGCTGGGAGACTCTGGGACTGTCCTGGGAATGGCCCTGA
GGAGCCACGACCGCAGCACCAGGCCCCTCTACATCTCCGTGGGCCACAGGATGAGCCTGGAG
GCCGCTGTGCGCCTGACTTGCTGCTGCTGCAGGTTCCGGATCCCAGAGCCCGTGCGCCAGGC
TGACATCTGCTCCCGAGAGCACATCCGCAAGTCGCTGGGACTCCCCGGGCCACCCACACCGA
GGAGCCCGAAGGCGCAGAGGCCAGTGGCATGCCCCAAAGGAGACTCCGGAGAGTCCTCAGCA
CTTTGT**TGA**ACGTGGTGGTGAGAGCACACGTCCTCGTCTCATTCCTGATCGAACGCGGTGGT
GAGAGCACACGTCCTCGTCTCGTTCCTGATCGAACGCGGTGGTGAGAGCA

MALEAAGGPPEETLSLWKREQARLKAHVVDRDTEAWQRDPAFSG
LQRVGGVDVSFVKGDSVRACASLVVLSFPELEVVYEESRMVSLTAPYVSGFLAFREVP
FLLELVQQLREKEPGLMPQVLLVDGNGVLHHRGFGVACHLGVLTDLPCVGVAKKLLQV
DGLENNALHKEKIRLLQTRGDSFPLLGDSGTVLGMALRSHDRSTRPLYISVGHRMSLE
AAVRLTCCCCRFRIPEPVRQADICSREHIRKSLGLPGPPTPRSPKAQRPVACPKGDSG
ESSALC

Homo sapiens endonuclease V transcript variant 2, mRNA

NCBI Reference Sequence: NM_001164637.1

Without exon 3 and short exon 9 + exon 10

>gi|257467547|ref|NM_001164637.1| Homo sapiens endonuclease V (ENDOV), transcript variant 2, mRNA

GTGCGGAAGGGGTGCCCGGGACGAAGCC**ATG**GCCCTGGAGGCGGCGGGAGGGCCGCCGGAGG
AAACGCTGTCACTGTGGAAACGGGAGCAAGCTCGGCTGAAGGCCCACGTCGTAGACCGGGAC
ACCGAGGCGTGGCAGCGAGACCCCGCCTTCTCGGGTCTGCAGAGGGTCGGGGGCGTTGACGT
GTCCTTCGTGAAAGGGGACAGTGTCCGCGCTTGTGCTTCCCTGGTGGTGCTCAGCTTCCCTG
AGCTCGAGGTCCTTCTTGTGGATGGAAACGGGGTACTCCACCACCGAGGCTTTGGGGTGGCC
TGCCACCTTGGCGTCCTTACAGACCTGCCGTGTGTTGGGGTGGCCAAGAAACTTCTGCAGGT
GGATGGGCTGGAGAACAACGCCCTGCACAAGGAGAAGATCCGACTCCTGCAGACTCGAGGAG
ACTCATTCCCTCTGCTGGGAGACTCTGGGACTGTCCTGGGAATGGCCCTGAGGAGCCACGAC
CGCAGCACCAGGCCCCTCTACATCTCCGTGGGCCACAGGATGAGCCTGGAGGCCGCTGTGCG
CCTGACTTGCTGCTGCTGCAGGTTCCGGATCCCAGAGCCCGTGCGCCAGGCTGACATCTGCT
CCCGAGAGCACATCCGCAAGTCGCTGGGACTCCCCGGGCCACCCACACCGAGGAGCCCGAAG
GCGCAGAGGCCAGTGGCATGCCCCAAAGGAGACTCCGGAGAGTCCTCAG*CACTTTGT****TGA***AC
GTGGTGGTGAGAGCACACGTCCTCGTCTCATTCCTGATCGAACGCGGTGGTGAGAGCACACG
TCCTCGTCTCGTTCCTGATCGAACGCGGTGGTGA

MALEAAGGPPEETLSLWKREQARLKAHVVDRDTEAWQRDPAFSG
LQRVGGVDVSFVKGDSVRACASLVVLSFPELEVLLVDGNGVLHHRGFGVACHLGVLTD
LPCVGVAKKLLQVDGLENNALHKEKIRLLQTRGDSFPLLGDSGTVLGMALRSHDRSTR
PLYISVGHRMSLEAAVRLTCCCCRFRIPEPVRQADICSREHIRKSLGLPGPPTPRSPK
AQRPVACPKGDSGESSALC

Homo sapiens endonuclease V, transcript variant 3, mRNA

NCBI Reference Sequence: NM_001164638.1

Without exon 3 and with full-length exon 9

>gi|257467549|ref|NM_001164638.1| Homo sapiens endonuclease V (ENDOV), transcript variant 3, mRNA

GTGCGGAAGGGGTGCCCGGGACGAAGCC**ATG**GCCCTGGAGGCGGCGGGAGGGCCGCCGGAGG
AAACGCTGTCACTGTGGAAACGGGAGCAAGCTCGGCTGAAGGCCCACGTCGTAGACCGGGAC
ACCGAGGCGTGGCAGCGAGACCCCGCCTTCTCGGGTCTGCAGAGGGTCGGGGGCGTTGACGT
GTCCTTCGTGAAAGGGGACAGTGTCCGCGCTTGTGCTTCCCTGGTGGTGCTCAGCTTCCCTG
AGCTCGAGGTCCTTCTTGTGGATGGAAACGGGGTACTCCACCACCGAGGCTTTGGGGTGGCC
TGCCACCTTGGCGTCCTTACAGACCTGCCGTGTGTTGGGGTGGCCAAGAAACTTCTGCAGGT
GGATGGGCTGGAGAACAACGCCCTGCACAAGGAGAAGATCCGACTCCTGCAGACTCGAGGAG
ACTCATTCCCTCTGCTGGGAGACTCTGGGACTGTCCTGGGAATGGCCCTGAGGAGCCACGAC
CGCAGCACCAGGCCCCTCTACATCTCCGTGGGCCACAGGATGAGCCTGGAGGCCGCTGTGCG
CCTGACTTGCTGCTGCTGCAGGTTCCGGATCCCAGAGCCCGTGCGCCAGGCTGACATCTGCT
CCCGAGAGCACATCCGCAAGTCGCTGGGACTCCCCGGGCCACCCACACCGAGGAGCCCGAAG
GCGCAGAGGCCAGTGGCATGCCCCAAAGGAGACTCCGGAGAGTCCTCAG*GTGAGGGCCAGCC*
CCCACAGGACCACAGCCCAGGCCCCAGGACAGCCCCAAGGCCAGGCTCCCAGGAGCAGGCGG
*GCAAGGACTGGCAG**TAG***GGTGGAACTGGGCACCATGAAGACAAGAAGGCCACCGGCCACCCC
GTTCTGGCCTCAGGACACTGACCACCCCTGGGGGTGGTCTAG

MALEAAGGPPEETLSLWKREQARLKAHVVDRDTEAWQRDPAFSG
LQRVGGVDVSFVKGDSVRACASLVVLSFPELEVLLVDGNGVLHHRGFGVACHLGVLTD
LPCVGVAKKLLQVDGLENNALHKEKIRLLQTRGDSFPLLGDSGTVLGMALRSHDRSTR
PLYISVGHRMSLEAAVRLTCCCCRFRIPEPVRQADICSREHIRKSLGLPGPPTPRSPK
AQRPVACPKGDSGESSGEGQPPQDHSPGPRTAPRPGSQEQAGKDW

Appendix II: Raw data for MTT-assay

Early transformed MEF cell treated with CPT

Table A. Comparison between the different MEF WT cell lines (relative values).

CPT (µM)	0	0,1	0,5	1	2	3	5	n
WT #2	100	79,0	69,1	63,7	51,6			2
WT #3	100	56,9	36,7	30,1	25,2	2,3	3,1	5
WT #5	100	58,7	35,0	30,8	25,8	41,0	38,5	5
WT #6	100	66,7	50,6	44,9	45,5			3
Average	100	65,3	47,8	42,4	37,0	21,6	20,8	
STDEV		10,0	15,8	15,7	13,5	27,3	25,0	

Table B. Comparison between the different MEF KO cell lines (relative values).

CPT (µM)	0	0,1	0,5	1	2	3	5	n
KO #2	100	69,9	53,6	45,0	37,7	35,3	27,1	5
KO #3	100	45,2	25,6	18,5	14,9			3
KO #4	100	68,8	50,8	41,1	34,0	33,0	29,0	5
KO #5	100	47,4	18,5	10,7	7,8	9,4	8,8	5
Average	100	57,8	37,1	28,8	23,6	25,9	21,6	
STDEV		13,3	17,7	16,8	14,5	14,4	11,2	

Table C. Comparison between MEF WT and KO (relative values).

WT	0	0,1	0,5	1	2	3	5
Average	100	65,3	47,8	42,4	37,0	21,6	20,8
STDEV		10,0	15,8	15,7	13,5	28,6	31,7
KO	**0**	**0,1**	**0,5**	**1**	**2**	**3**	**5**
Average	100	57,8	37,1	28,8	23,6	25,9	21,6
STDEV		13,3	17,7	16,8	14,5	14,4	11,2

Primary MEF cell treated with CPT

Table D. Comparison between the different MEF WT cell lines (relative values).

CPT (µM)	0	0,05	0,1	0,5	1	2	4	6	n
WT #2	100	86,2	74,2	62,1	46,9	41,9	37,8		2
WT #3	100	86,9	82,0	71,6	55,0		41,9	43,4	5
WT #4	100	79,1	69,6	46,3	36,4	34,3	34,6		2
WT #5	100	65,4	62,9	48,6	40,5		29,1	29,7	5
WT #6	100	57,8	52,8	42,2	36,3		26,8	28,5	4
Average	100	75,1	68,3	54,2	43,0	38,1	34,0	33,8	
STDEV		12,9	11,1	12,3	8,0	5,4	6,2	8,3	

Table E. Comparison between the different MEF KO cell lines (relative values).

CPT (µM)	0	0,05	0,1	0,5	1	2	4	6	n
KO #2	100	78,6	71,7	57,0	41,6	35,3	37,8		3
KO #3	100	63,9	60,0	45,3	32,6		18,6	19,4	5
KO #4	100	77,5	70,7	46,4	35,5	29,4	29,0		2
KO #5	100	62,4	56,6	44,3	31,7		19,3	20,7	5
KO #6	100	69,8	65,7	55,8	49,2		37,0	38,7	4
Average	100	70,4	64,9	49,8	38,1	32,3	28,3	26,3	
STDEV		7,5	6,6	6,1	7,3	4,2	9,2	10,8	

Table F. Comparison between MEF WT and KO (relative values).

WT	0	0,05	0,1	0,5	1	2	4	6
Average	100	75,1	68,3	54,2	43,0	38,1	34,0	33,8
STDEV		12,9	11,1	12,3	8,0	5,4	6,2	8,3
KO	**0**	**0,05**	**0,1**	**0,5**	**1**	**2**	**4**	**6**
Average	100	70,4	64,9	49,8	38,1	32,3	28,3	26,3
STDEV		7,5	6,6	6,1	7,3	4,2	9,2	10,8

Primary MEF cell treated with MMS, MMC and gamma radiation

Table G. Comparison between MEF WT and KO treated with MMS (µM) (relative values).

WT	**0**	**50**	**100**	**120**	**140**	**180**	**200**
Average	100	82,1	80,2	73,3	66,4	55,3	34,8
STDEV		6,8	4,6	7,5	2,6	4,4	2,6
KO	**0**	**50**	**100**	**120**	**140**	**180**	**200**
Average	100	83,4	77,1	75,0	67,0	55,6	46,3
STDEV		4,0	7,3	9,5	8,1	8,3	1,9

Table H. Comparison between MEF WT and KO treated with MMC (µM) (relative values).

WT	**0**	**0,1**	**0,5**	**1**	**5**	**10**	**20**
Average	100	89,3	84,4	80,8	70,0	51,6	37,5
STDEV		3,5	3,4	6,4	7,2	2,2	3,3
KO	**0**	**0,1**	**0,5**	**1**	**5**	**10**	**20**
Average	100	85,3	81,2	78,9	66,5	46,6	34,8
STDEV		4,1	5,8	5,3	3,8	2,7	0,7

Table I. Comparison between MEF WT and KO irradiated with gamma (Gy) (relative values).

WT	**0**	**20**	**40**	**60**
Average	100	93,0	82,4	78,5
STDEV		6,1	2,2	0,2
KO	**0**	**20**	**40**	**60**
Average	100	89,2	84,1	73,8
STDEV		5,4	1,8	1,1

Appendix III: Multiple sequence alignments

Mulltiple sequence alignment of endonuclease V proteins from different organisms

Key catalytic residues are indicated by black arrows and the residues forming the binding pocket are indicated by blue arrows.

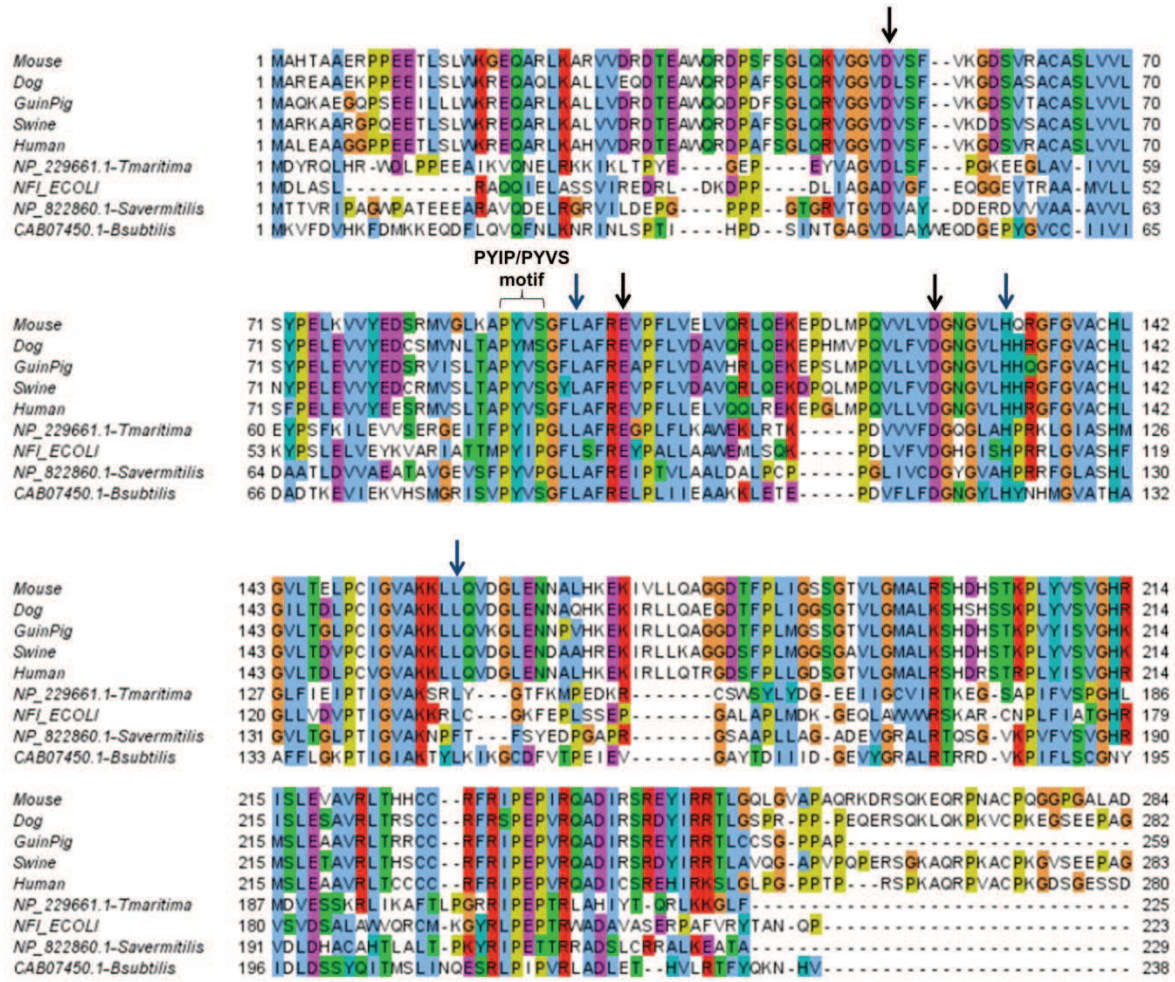

Figure A. Multiple sequence alignment of Endonuclease V proteins from different organisms. Mouse: *Mus musculus*, dog: *Canis familiaris*, GuinPig: *Cavia porcellus*, Swine: *Sus scrofa*, Human: *Homo sapiens*, NP_229661.1-Tmaritima: *Thermotoga maritima*, NFI_ECOLI: *Escherichia coli*, NP_822860.1Savermitilis: *Streptomyces avermitilis*, and CAB0750.1Bsubtilis: *Bacillus subtilis.* (J.K. Lærhahl, unpublished data).

Multiple sequence alignment of endonuclease V proteins from different mammals

Figure B. Multiple sequence alignment of Endonuclease V proteins from the mammalian organisms mouse (*Mus musculus*), rat (*Rattus norvegicus*), dog (*Canis familiaris*), gorilla (*Gorilla gorilla*), guinea pig (*Cavia porcellus*), orangutan (*Pongo pygmaeus*), pig (*Sus scrofa*), tenrec (*Ecinops telfairi*) and human (*Homo sapiens*) (J.K. Lærhahl, unpublished data).

Appendix IV: Vector maps

Vector map of pEGFP-N1 from Clontech

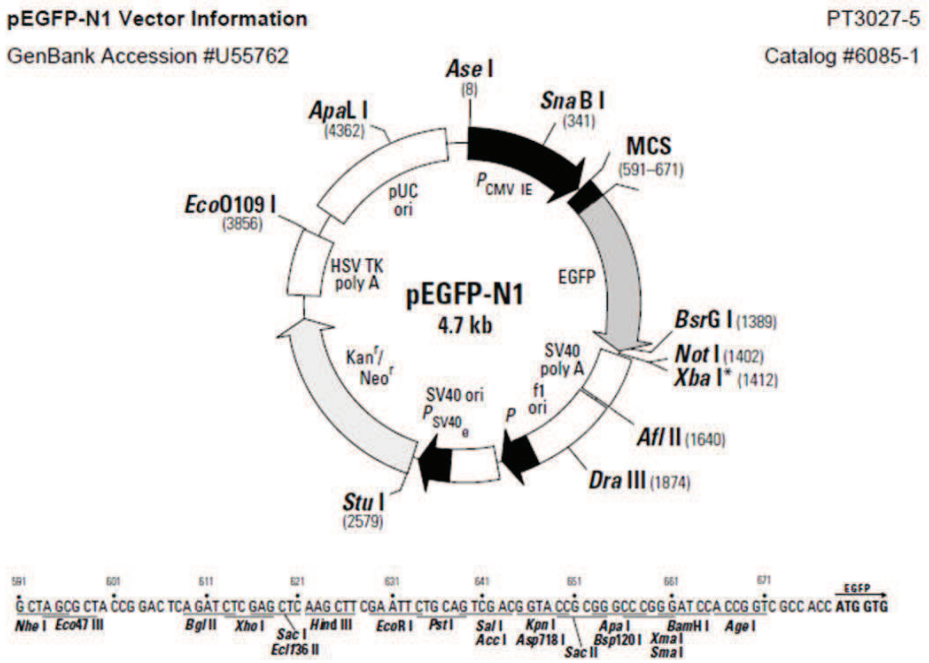

Vector map pEGFP-C1 from Clontech

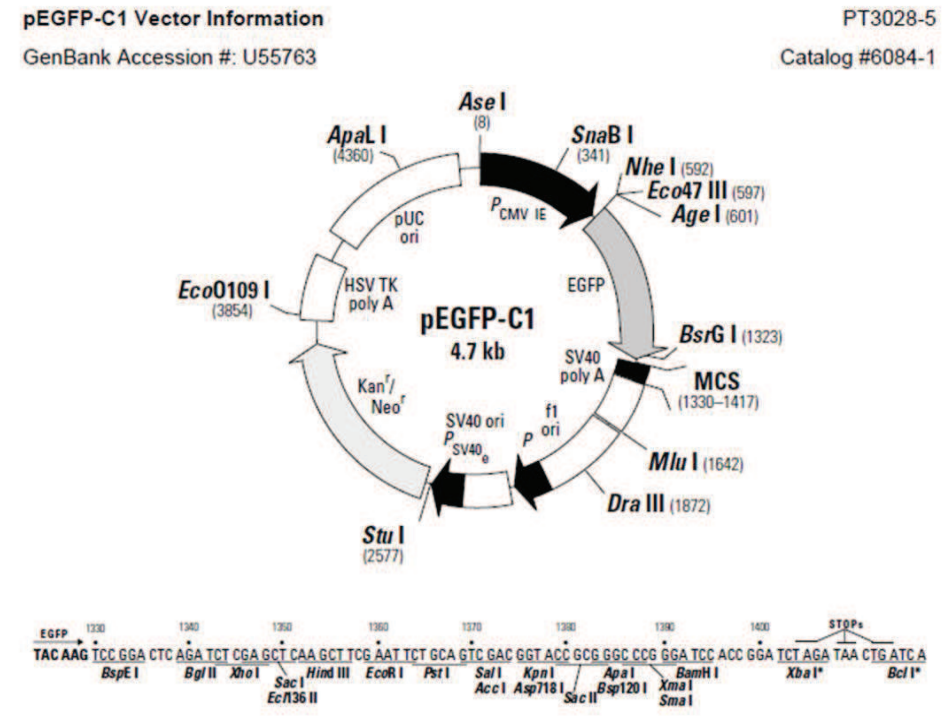

Units of measurements

°C	Degrees Celcius	mg	Milligram (10^{-3} g)
g	Gram	ml	Millilitre (10^{-3} L)
g	G force	mM	Millimolar (10-^{3} M)
kb	Kilobases (10^{3} b)	nm	Nanometer (10^{-9} m)
kDa	Kilo Dalton (10^{3} Da)	ng	Nanogram (10^{-9} g)
L	Litre	µg	Microgram (10^{-6} g)
M	Molar	µl	Microlitre (10^{-6} L)
		V	Volt